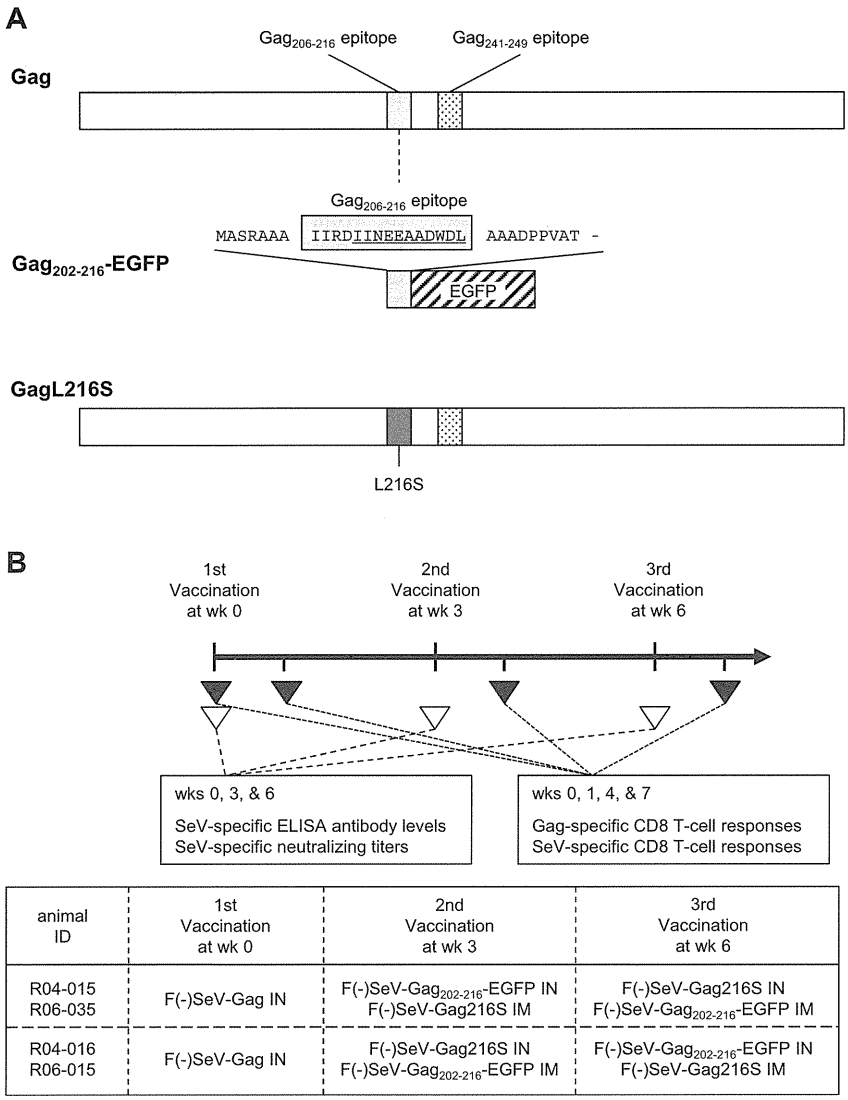

animal ID	1st Vaccination at wk 0	2nd Vaccination at wk 3	3rd Vaccination at wk 6
R04-015 R06-035	F(-)SeV-Gag IN	F(-)SeV-Gag$_{202-216}$-EGFP IN F(-)SeV-Gag216S IM	F(-)SeV-Gag216S IN F(-)SeV-Gag$_{202-216}$-EGFP IM
R04-016 R06-015	F(-)SeV-Gag IN	F(-)SeV-Gag216S IN F(-)SeV-Gag$_{202-216}$-EGFP IM	F(-)SeV-Gag$_{202-216}$-EGFP IN F(-)SeV-Gag216S IM

Fig. 1. Vaccination protocols. (A) Inserts of F(-)SeV vectors used for vaccination. F(-)SeV-Gag, F(-)SeV-Gag$_{202-216}$-EGFP, and F(-)SeV-Gag216S express the SIVmac239 Gag, a Gag$_{202-216}$-EGFP fusion protein, and a mutant Gag with a leucine-to-serine substitution at the 216th amino acid (L216S), respectively. The L216S substitution results in escape from Gag$_{206-216}$-specific CD8$^+$ T-cell recognition. (B) Protocols for macaque vaccination. Four *90-120-Ia*-positive macaques received F(-)SeV-Gag intranasally (IN) at the first vaccination. Macaques R04-015 and R06-035 received F(-)SeV-Gag$_{202-216}$-EGFP IN and F(-)SeV-Gag216S intramuscularly (IM) at the second vaccination and vice versa at the third. Macaques R04-016 and R06-015 received F(-)SeV-Gag216S IN and F(-)SeV-Gag$_{202-216}$-EGFP IM at the second vaccination and vice versa at the third.

(BD, Tokyo, Japan) and the following monoclonal antibodies: fluorescein isothiocyanate (FITC)-conjugated anti-human CD4 (BD, #556615, M-T477), peridinin chlorophyll protein (PerCP)-conjugated anti-human CD8 (BD, #347314, SK1), allophycocyanin (APC)-conjugated anti-human CD3 (BD, #557597, SP34-2), and phycoerythrin (PE)-conjugated anti-human IFN-γ antibodies (BD, #557074, 4S.B3). Specific CD8$^+$ T-cell levels were calculated by subtracting non-specific IFN-γ$^+$ CD8$^+$ T-cell frequencies from those after Gag epitope peptide-specific or SeV-specific stimulation. Specific CD8$^+$ T-cell levels lower than 100 per million PBMCs were considered negative.

2.4. Measurement of anti-SeV IgG levels

The plasma anti-SeV immunoglobulin G (IgG) levels were measured by an enzyme-linked immunosorbent assay (ELISA) (Denka Seiken, Tokyo, Japan) using whole inactivated SeV (HVJ Z strain) particles and a peroxidase-conjugated anti-monkey IgG antibody [30].

2.5. Measurement of anti-SeV neutralizing titers

We measured plasma SeV-specific neutralizing titers on LLC-MK2 cells using a recombinant SeV expressing enhanced

green fluorescent protein (SeV-EGFP) as described before [31]. We determined the end-point plasma titers required for 10-fold reduction of SeV-EGFP infectivity compared to the negative control without plasma (90% neutralization titer; 90% effective concentration [EC_{90}]).

3. Results

3.1. Antigen-specific $CD8^+$ T-cell responses after repeated F(-)SeV vector vaccination

We used four SIV controllers possessing the MHC-I haplotype *90-120-Ia* [22,24]. In these rhesus macaques that were vaccinated and challenged with SIV in our previous studies [25,27], plasma viremia was undetectable in the chronic phase. In the present study, these four animals received SeV vector vaccination three times with intervals of three weeks in the chronic phase. Three kinds of SeV vectors, F(-)SeV-Gag inducing both $Gag_{206-216}$ epitope-specific and $Gag_{241-249}$ epitope-specific $CD8^+$ T-cell responses, F(-)SeV-$Gag_{202-216}$-EGFP inducing the former, and F(-)SeV-Gag216S inducing the latter, were used for the vaccination (Fig. 1). All four macaques received an intranasal F(-)SeV-Gag vector inoculation at the first vaccination. Macaques R04-015 and R06-035 received F(-)SeV-$Gag_{202-216}$-EGFP intranasally and F(-)SeV-Gag216S intramuscularly at the second vaccination and vice versa at the third. Macaques R04-016 and R06-015 received F(-)SeV-Gag216S intranasally and F(-)SeV-$Gag_{202-216}$-EGFP intramuscularly at the second vaccination and vice versa at the third.

Previously, macaques possessing the MHC-I haplotype *90-120-Ia* were shown to induce $Gag_{206-216}$ and $Gag_{241-249}$ epitope-specific $CD8^+$ T-cell responses dominantly in the early phase after SIVmac239 challenge [25,27]. In the present study, we examined these $Gag_{206-216}$-specific and $Gag_{241-249}$-specific $CD8^+$ T-cell responses one week after each vaccination (Fig. 2). The first F(-)SeV-Gag vaccination enhanced both $Gag_{206-216}$-specific and $Gag_{241-249}$-specific $CD8^+$ T-cell responses in macaques R06-035 and R06-015 but not in R04-016. In macaque R04-015, efficient $Gag_{206-216}$-specific and $Gag_{241-249}$-specific $CD8^+$ T-cell responses were detected at week 1 after the first vaccination, while PBMC samples were unavailable for analysis of responses just before the first vaccination.

At week 4, one week after the second vaccination, animals had similar or higher $Gag_{206-216}$-specific and $Gag_{241-249}$-specific $CD8^+$ T-cell frequencies compared to those at week 1. Also at week 7, one week after the third vaccination, animals had similar or higher $Gag_{206-216}$-specific and $Gag_{241-249}$-specific $CD8^+$ T-cell frequencies compared to those at week 4. Enhancement of these Gag-specific $CD8^+$ T-cell response was clear after the second vaccination (at week 4) in macaques R04-016 and R06-035 and after the third vaccination (at week 7) in macaques R04-015 and R06-015. Thus, all four animals showed higher Gag-specific $CD8^+$ T-cell responses at week 7 compared to those at week 1, indicating enhancement of Gag-specific $CD8^+$ T-cell responses by the second/third vaccination.

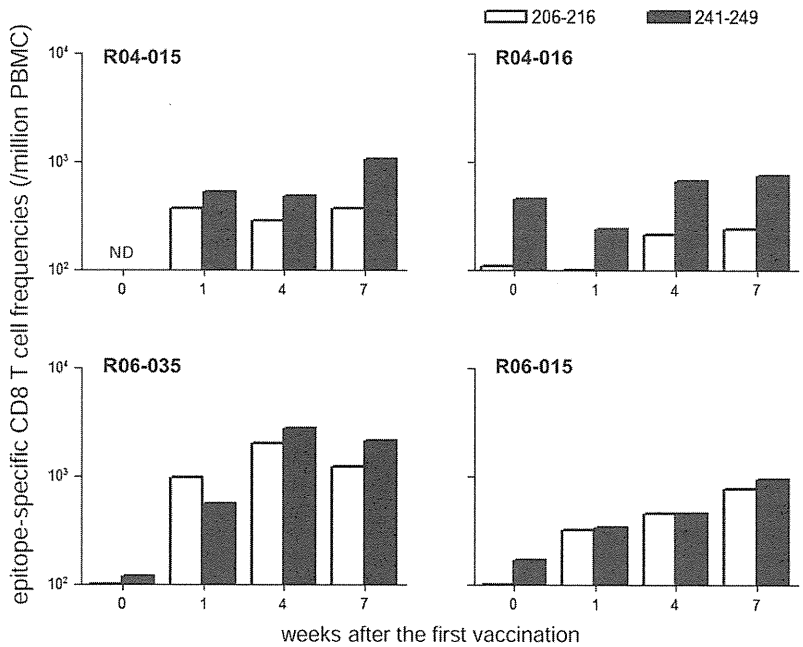

Fig. 2. Gag epitope-specific $CD8^+$ T-cell responses after repeated SeV vector vaccination. $Gag_{206-216}$-specific (open boxes) and $Gag_{241-249}$-specific (closed boxes) $CD8^+$ T-cell responses at week 0 (just before the first vaccination) and at weeks 1, 4, and 7 after the first vaccination (one week after each vaccination) were examined. ND, not determined.

3.2. SeV-specific CD8$^+$ T-cell responses after repeated F(-)SeV vector vaccination

We also examined SeV-specific CD8$^+$ T-cell responses one week after each vaccination (Fig. 3). SeV-specific CD8$^+$ T-cell responses were undetectable at week 0, just before the first vaccination. Vaccination mostly enhanced SeV-specific CD8$^+$ T-cell responses, and all animals showed efficient SeV-specific CD8$^+$ T-cell responses after three times of vaccination. Clear difference in the patterns of enhancement was not observed between $Gag_{206-216}$/$Gag_{241-249}$-specific and SeV-specific CD8$^+$ T-cell responses, suggesting little or no change in the immunodominance patterns between these CD8$^+$ T-cell responses by the second/third SeV vector vaccination.

3.3. SeV-specific antibody responses at repeated F(-)SeV vector vaccination

We then examined SeV-specific antibody responses just before each vaccination (Fig. 4 and Fig. 5). While these animals received a single SeV vector vaccination in previous studies more than a year before, ELIZA showed marginal levels of SeV-specific antibodies at week 0, just before the first vaccination. These animals exhibited undetectable or low levels of SeV-specific neutralizing antibody responses at week 0. At weeks 3 and 6, just before the second/third vaccination, all four animals had high levels of SeV-specific IgGs and neutralizing titers, indicating that the second/third SeV vector vaccination enhanced Gag-specific CD8$^+$ T-cell responses in the presence of high levels of SeV-specific neutralizing responses.

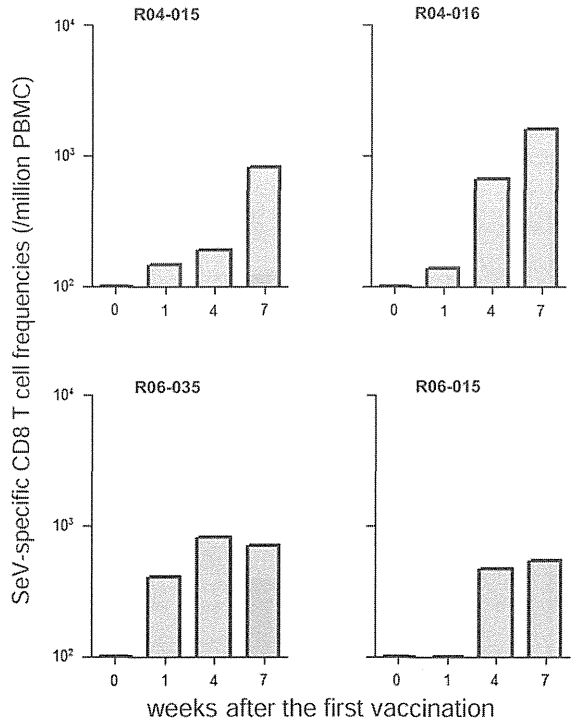

Fig. 3. SeV-specific CD8$^+$ T-cell responses after repeated SeV vector vaccination. SeV-specific CD8$^+$ T-cell responses at week 0 (just before the first vaccination) and at weeks 1, 4, and 7 after the first vaccination (one week after each vaccination) were examined.

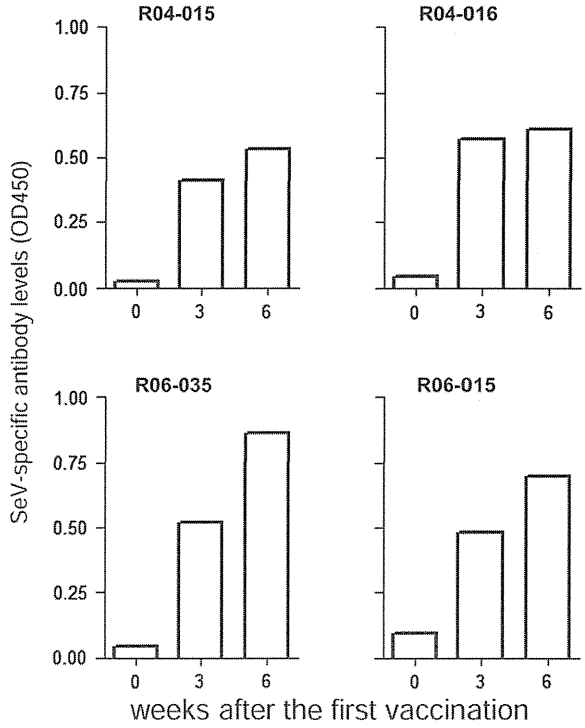

Fig. 4. SeV-specific IgG levels in plasma at repeated SeV vector vaccination. Plasma samples obtained at weeks 0, 3, and 6 after the first vaccination (just before each vaccination) were subjected to ELISA assay. OD450, optical density at 450 nm.

4. Discussion

Replication-defective viral vectors are promising safe tools for eliciting antigen-specific T-cell responses. A single inoculation of these vectors can induce efficient T-cell responses, which would peak within a couple of weeks and decline after that, although durable T-cell memory induction is important for vaccine efficacy. In the present study, we examined immunogenicity of three times of replication-defective SeV vector vaccination with intervals of three weeks in macaques and showed that antigen-specific CD8$^+$ T-cell responses after the third vaccination were higher than those after the first vaccination. Our results indicate the potential of repeated SeV vector vaccination to induce efficient and durable T-cell responses, providing a solution toward durable vaccine efficacy.

CD8$^+$ T-cells recognize MHC-I-restricted epitopes presented on target cells, and animals sharing MHC-I alleles would be useful for exact evaluation of vaccine immunogenicity. We confirmed $Gag_{206-216}$-specific and $Gag_{241-249}$-specific CD8$^+$ T-cell responses in macaques R04-015, R04-

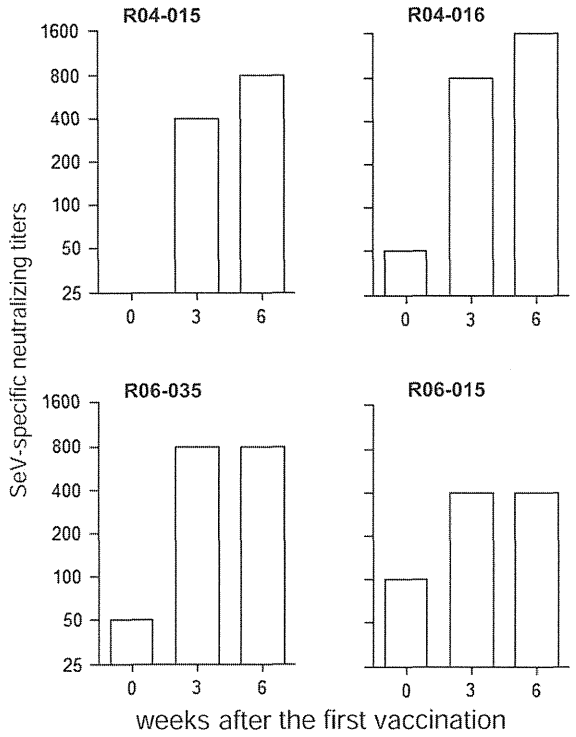

Fig. 5. SeV-specific neutralizing titers in plasma at repeated SeV vector vaccination. Plasma samples obtained at weeks 0, 3, and 6 after the first vaccination (just before each vaccination) were subjected to anti-SeV neutralizing assay. The end-point plasma titers required for 10-fold reduction of SeV-EGFP infectivity are shown.

016, R06-015, and R06-035 sharing MHC-I haplotype *90-120-Ia* after SIVmac239 challenge in our previous studies [25–27]. Then, we have focused on analyzing $Gag_{206-216}$-specific and $Gag_{241-249}$-specific $CD8^+$ T-cell responses for evaluation of vaccine immunogenicity in the present study.

Previous studies have shown that Gag-specific $CD8^+$ T-cell frequencies peaked around one week after a single F(-)SeV-Gag vaccination [19]. Indeed, Gag-specific $CD8^+$ T-cell responses became undetectable in a few months in five of six F(-)SeV-Gag-boosted macaques [32]. Then, it is inferred that $Gag_{206-216}$-specific and $Gag_{241-249}$-specific $CD8^+$ T-cell frequencies would be much lower at weeks 4 and 7 than those at week 1 without repeated vaccination. In the present study, however, those frequencies at week 7 were higher than at week 1. $Gag_{206-216}$-specific and $Gag_{241-249}$-specific $CD8^+$ T-cell frequencies at weeks 4 and 7 were similar or rather higher than those at weeks 1 and 4, respectively. These results imply that each of the second and the third vaccination enhanced these $CD8^+$ T-cell responses, leading to augmented, durable $Gag_{206-216}$-specific and $Gag_{241-249}$-specific $CD8^+$ T-cell responses.

Pre-existing anti-vector antibodies can be an obstacle to the immunogenicity of viral vectors [15,33–35]. Viral vector vaccination induces immune responses against the vector virus itself, and so, anti-vector antibodies could inhibit induction of antigen-specific T-cell responses by repeated vaccination. Indeed, after the first vaccination, all four animals had high levels of SeV-specific neutralizing antibodies, which may have affected efficacy of T-cell induction by the second and the third SeV vector vaccination with short intervals. However, the second and the third SeV vector vaccination in the presence of high levels of SeV-specific neutralizing antibodies enhanced $Gag_{206-216}$-specific and $Gag_{241-249}$-specific $CD8^+$ T-cell responses.

Recently, we showed that intranasal SeV vector immunization is more immunogenic than intramuscular in the presence of SeV-specific neutralizing antibodies [20]. In that study, Gag-specific $CD8^+$ T-cell responses were induced not by intramuscular but by intranasal immunization with 6×10^8 CIU of F(-)SeV-Gag vectors in the presence of 1:100 of plasma SeV-specific neutralizing titers. We were unable to quantify SeV-specific IgA levels. In the present study, however, clear difference in immunogenicity was not shown between intranasal and intramuscular SeV vector vaccination. Enhancement of antigen-specific $CD8^+$ T-cell responses by the second, intramuscular vaccination was observed in macaques R04-016 and R06-035 (Fig. 2). Intramuscular immunization with higher doses (6×10^9 CIU) may overcome the inhibitory effect by SeV-specific neutralizing antibodies.

In summary, we examined antigen-specific $CD8^+$ T-cell responses in macaques after three times of SeV vector vaccination with intervals of three weeks. Antigen-specific $CD8^+$ T-cell responses did not decline but were enhanced by the second and the third vaccination even in the presence of high levels of SeV-specific neutralizing antibodies. These results indicate that repeated SeV vector vaccination even with short intervals can contribute to induction of efficient, durable T-cell responses.

Acknowledgments

This work was supported by grants from the Ministry of Education, Culture, Sports, Science, and Technology, grants from the Ministry of Health, Labor, and Welfare, and a grant from Takeda Science Foundation in Japan. We thank T. Kamada for his help and H. Akari, Y. Yasutomi, F. Ono, A. Hiyaoka, K. Komatsuzaki, and K. Oto for their assistance in animal experiments.

References

[1] R.A. Koup, J.T. Safrit, Y. Cao, C.A. Andrews, G. McLeod, W. Borkowsky, C. Farthing, D.D. Ho, Temporal association of cellular immune responses with the initial control of viremia in primary human immunodeficiency virus type 1 syndrome, J. Virol. 68 (1994) 4650–4655.

[2] P. Borrow, H. Lewicki, B.H. Hahn, G.M. Shaw, M.B. Oldstone, Virus-specific $CD8^+$ cytotoxic T-lymphocyte activity associated with control of viremia in primary human immunodeficiency virus type 1 infection, J. Virol. 68 (1994) 6103–6110.

[3] T. Matano, R. Shibata, C. Siemon, M. Connors, H.C. Lane, M.A. Martin, Administration of an anti-CD8 monoclonal antibody interferes with the clearance of chimeric simian/human immunodeficiency virus during primary infections of rhesus macaques, J. Virol. 72 (1998) 164–169.

[4] X. Jin, D.E. Bauer, S.E. Tuttleton, S. Lewin, A. Gettie, J. Blanchard, C.E. Irwin, J.T. Safrit, J. Mittler, L. Weinberger, L.G. Kostrikis, L. Zhang, A.S. Perelson, D.D. Ho, Dramatic rise in plasma viremia after $CD8^+$ T cell depletion in simian immunodeficiency virus-infected macaques, J. Exp. Med. 189 (1999) 991–998.

[5] J.E. Schmitz, M.J. Kuroda, S. Santra, V.G. Sasseville, M.A. Simon, M.A. Lifton, P. Racz, K. Tenner-Racz, M. Dalesandro, B.J. Scallon, J. Ghrayeb, M.A. Forman, D.C. Montefiori, E.P. Rieber, N.L. Letvin, K.A. Reimann, Control of viremia in simian immunodeficiency virus infection by $CD8^+$ lymphocytes, Science 28 (1999) 857–860.

[6] R.A. Seder, A.V. Hill, Vaccines against intracellular infections requiring cellular immunity, Nature 406 (2000) 793–798.

[7] P.J. Goulder, D.I. Watkins, HIV and SIV CTL escape: implications for vaccine design, Nat. Rev. Immunol. 4 (2004) 630–640.

[8] A.J. McMichael, T. Hanke, HIV vaccines 1983–2003, Nat. Med. 9 (2003) 874–880.

[9] R.R. Amara, F. Villinger, J.D. Altman, S.L. Lydy, S.P. O'Neil, S.I. Staprans, D.C. Montefiori, Y. Xu, J.G. Herndon, L.S. Wyatt, M.A. Candido, N.L. Kozyr, P.L. Earl, J.M. Smith, H.L. Ma, B.D. Grimm, M.L. Hulsey, J. Miller, H.M. McClure, J.M. McNicholl, B. Moss, H.L. Robinson, Control of a mucosal challenge and prevention of AIDS by a multiprotein DNA/MVA vaccine, Science 292 (2001) 69–74.

[10] J.W. Shiver, T.M. Fu, L. Chen, D.R. Casimiro, M.E. Davies, R.K. Evans, Z.Q. Zhang, A.J. Simon, W.L. Trigona, S.A. Dubey, L. Huang, V.A. Harris, R.S. Long, X. Liang, L. Handt, W.A. Schleif, L. Zhu, D.C. Freed, N.V. Persaud, L. Guan, K.S. Punt, A. Tang, M. Chen, K.A. Wilson, K.B. Collins, G.J. Heidecker, V.R. Fernandez, H.C. Perry, J.G. Joyce, K.M. Grimm, J.C. Cook, P.M. Keller, D.S. Kresock, H. Mach, R.D. Troutman, L.A. Isopi, D.M. Williams, Z. Xu, K.E. Bohannon, D.B. Volkin, D.C. Montefiori, A. Miura, G.R. Krivulka, M.A. Lifton, M.J. Kuroda, J.E. Schmitz, N.L. Letvin, M.J. Caulfield, A.J. Bett, R. Youil, D.C. Kaslow, E.A. Emini, Replication-incompetent adenoviral vaccine vector elicits effective anti-immunodeficiency-virus immunity, Nature 415 (2002) 331–335.

[11] X. Jin, M. Ramanathan Jr., S. Barsoum, G.R. Deschenes, L. Ba, J. Binley, D. Schiller, D.E. Bauer, D.C. Chen, A. Hurley, L. Gebuhrer, R. El Habib, P. Caudrelier, M. Klein, L. Zhang, D.D. Ho, M. Markowitz, Safety and immunogenicity of ALVAC vCP1452 and recombinant gp160 in newly human immunodeficiency virus type 1-infected patients treated with prolonged highly active antiretroviral therapy, J. Virol. 76 (2002) 2206–2216.

[12] S.G. Hansen, C. Vieville, N. Whizin, L. Coyne-Johnson, D.C. Siess, D.D. Drummond, A.W. Legasse, M.K. Axthelm, K. Oswald, C.M. Trubey, M.J. Piatak, J.D. Lifson, J.A. Nelson, M.A. Jarvis, L.J. Picker, Effector memory T cell responses are associated with protection of rhesus monkeys from mucosal simian immunodeficiency virus challenge, Nat. Med. 15 (2009) 293–299.

[13] J. Liu, K.L. O'Brien, D.M. Lynch, N.L. Simmons, A. La Porte, A.M. Riggs, P. Abbink, R.T. Coffey, L.E. Grandpre, M.S. Seaman, G. Landucci, D.N. Forthal, D.C. Montefiori, A. Carville, K.G. Mansfield, M.J. Havenga, M.G. Pau, J. Goudsmit, D.H. Barouch, Immune control of an SIV challenge by a T-cell-based vaccine in rhesus monkeys, Nature 457 (2009) 87–91.

[14] J.L. Excler, C.L. Parks, J. Ackland, H. Rees, I.D. Gust, W.C. Koff, Replicating viral vectors as HIV vaccines: summary report from the IAVI sponsored satellite symposium at the AIDS vaccine 2009 conference, Biologicals 38 (2010) 511–521.

[15] S.F. Berkley, W.C. Koff, Scientific and policy challenges to development of an AIDS vaccine, Lancet 370 (2007) 94–101.

[16] A. Kato, Y. Sakai, T. Shioda, T. Kondo, M. Nakanishi, Y. Nagai, Initiation of Sendai virus multiplication from transfected cDNA or RNA with negative or positive sense, Genes Cells 1 (1996) 569–579.

[17] M. Kano, T. Matano, A. Kato, H. Nakamura, A. Takeda, Y. Suzaki, Y. Ami, K. Terao, Y. Nagai, Primary replication of a recombinant Sendai virus vector in macaques, J. Gen. Virol. 83 (2002) 1377–1386.

[18] H.O. Li, Y.F. Zhu, M. Asakawa, H. Kuma, T. Hirata, Y. Ueda, Y.S. Lee, M. Fukumura, A. Iida, A. Kato, Y. Nagai, M. Hasegawa, A cytoplasmic RNA vector derived from nontransmissible Sendai virus with efficient gene transfer and expression, J. Virol. 74 (2000) 6564–6569.

[19] T. Matano, M. Kobayashi, H. Igarashi, A. Takeda, H. Nakamura, M. Kano, C. Sugimoto, K. Mori, A. Iida, T. Hirata, M. Hasegawa, T. Yuasa, M. Miyazawa, Y. Takahashi, M. Yasunami, A. Kimura, D.H. O'Connor, D.I. Watkins, Y. Nagai, Cytotoxic T lymphocyte-based control of simian immunodeficiency virus replication in a preclinical AIDS vaccine trial, J. Exp. Med. 199 (2004) 1709–1718.

[20] C. Moriya, S. Horiba, K. Kurihara, T. Kamada, Y. Takahara, M. Inoue, A. Iida, H. Hara, T. Shu, M. Hasegawa, T. Matano, Intranasal Sendai viral vector vaccination is more immunogenic than intramuscular under pre-existing anti-vector antibodies, Vaccine 29 (2011) 8557–8563.

[21] M. Kato, H. Igarashi, A. Takeda, Y. Sasaki, H. Nakamura, M. Kano, T. Sata, A. Iida, M. Hasegawa, S. Horie, E. Higashihara, Y. Nagai, T. Matano, Induction of Gag-specific T-cell responses by therapeutic immunization with a Gag-expressing Sendai virus vector in macaques chronically infected with simian-human immunodeficiency virus, Vaccine 23 (2005) 3166–3173.

[22] T.K. Naruse, Z. Chen, R. Yanagida, T. Yamashita, Y. Saito, K. Mori, H. Akari, Y. Yasutomi, M. Miyazawa, T. Matano, A. Kimura, Diversity of MHC class I genes in Burmese-origin rhesus macaques, Immunogenetics 62 (2010) 601–611.

[23] M. Kawada, H. Igarashi, A. Takeda, T. Tsukamoto, H. Yamamoto, S. Dohki, M. Takiguchi, T. Matano, Involvement of multiple epitope-specific cytotoxic T-lymphocyte responses in vaccine-based control of simian immunodeficiency virus replication in rhesus macaques, J. Virol. 80 (2006) 1949–1958.

[24] T. Nomura, H. Yamamoto, T. Shiino, N. Takahashi, T. Nakane, N. Iwamoto, H. Ishii, T. Tsukamoto, M. Kawada, S. Matsuoka, A. Takeda, K. Terahara, Y. Tsunetsugu-Yokota, N. Iwata-Yoshikawa, H. Hasegawa, T. Sata, T.K. Naruse, A. Kimura, T. Matano, Association of major histocompatibility complex class I haplotypes with disease progression after simian immunodeficiency virus challenge in Burmese rhesus macaques, J. Virol. 86 (2012) 6481–6490.

[25] M. Kawada, T. Tsukamoto, H. Yamamoto, N. Iwamoto, K. Kurihara, A. Takeda, C. Moriya, H. Takeuchi, H. Akari, T. Matano, Gag-specific cytotoxic T-lymphocyte-based control of primary simian immunodeficiency virus replication in a vaccine trial, J. Virol. 82 (2008) 10199–10206.

[26] T. Tsukamoto, A. Takeda, T. Yamamoto, H. Yamamoto, M. Kawada, T. Matano, Impact of cytotoxic-T-lymphocyte memory induction without virus-specific $CD4^+$ T-Cell help on control of a simian immunodeficiency virus challenge in rhesus macaques, J. Virol. 83 (2009) 9339–9346.

[27] N. Iwamoto, T. Tsukamoto, M. Kawada, A. Takeda, H. Yamamoto, H. Takeuchi, T. Matano, Broadening of $CD8^+$ cell responses in vaccine-based simian immunodeficiency virus controllers, AIDS 24 (2010) 2777–2787.

[28] C. Moriya, H. Igarashi, A. Takeda, T. Tsukamoto, M. Kawada, H. Yamamoto, M. Inoue, A. Iida, T. Shu, M. Hasegawa, Y. Nagai, T. Matano, Abrogation of AIDS vaccine-induced cytotoxic T lymphocyte efficacy in vivo due to a change in viral epitope flanking sequences, Microbes. Infect. 10 (2008) 285–292.

[29] H.W. Kestler 3rd, D.J. Ringler, K. Mori, D.L. Panicali, P.K. Sehgal, M.D. Daniel, R.C. Desrosiers, Importance of the nef gene for maintenance of high virus loads and for development of AIDS, Cell 65 (1991) 651–662.

[30] M. Yoshizaki, T. Hironaka, H. Iwasaki, H. Ban, Y. Tokusumi, A. Iida, Y. Nagai, M. Hasegawa, M. Inoue, Naked Sendai virus vector lacking all of the envelope-related genes: reduced cytopathogenicity and immunogenicity, J. Gene. Med. 8 (2006) 1151–1159.

[31] C. Moriya, S. Horiba, M. Inoue, A. Iida, H. Hara, T. Shu, M. Hasegawa, T. Matano, Antigen-specific T-cell induction by vaccination with a recombinant Sendai virus vector even in the presence of vector-specific neutralizing antibodies in rhesus macaques, Biochem. Biophys. Res. Commun. 371 (2008) 850–854.

[32] A. Takeda, H. Igarashi, M. Kawada, T. Tsukamoto, H. Yamamoto, M. Inoue, A. Iida, T. Shu, M. Hasegawa, T. Matano, Evaluation of the

immunogenicity of replication-competent V-knocked-out and replication-defective F-deleted Sendai virus vector-based vaccines in macaques, Vaccine 26 (2008) 6839–6843.

[33] S.M. Sumida, D.M. Truitt, A.A.C. Lemckert, R. Vogels, J.H.H.V. Custers, M.M. Addo, S. Lockman, T. Peter, F.W. Peyerl, M.G. Kishko, S.S. Jackson, D.A. Gorgone, M.A. Lifton, M. Essex, B.D. Walker, J. Goudsmit, M.J.E. Havenga, D.H. Barouch, Neutralizing antibodies to adenovirus serotype 5 vaccine vectors are directed primarily against the adenovirus hexon protein, J. Immunol. 174 (2005) 7179–7185.

[34] A.T. Catanzaro, R.A. Koup, M. Roederer, R.T. Bailer, M.E. Enama, Z. Moodie, L. Gu, J.E. Martin, L. Novik, B.K. Chakrabarti, B.T. Butman, J.G. Gall, C.R. King, C.A. Andrews, R. Sheets, P.L. Gomez, J.R. Mascola, G.J. Nabel, B.S. Graham, Phase 1 safety and immunogenicity evaluation of a multiclade HIV-1 candidate vaccine delivered by a replication-defective recombinant adenovirus vector, J. Infect. Dis. 194 (2006) 1638–1649.

[35] F.H. Priddy, D. Brown, J. Kublin, K. Monahan, D.P. Wright, J. Lalezari, S. Santiago, M. Marmor, M. Lally, R.M. Novak, S.J. Brown, P. Kulkarni, S.A. Dubey, L.S. Kierstead, D.R. Casimiro, R. Mogg, M.J. Dinubile, J.W. Shiver, R.Y. Leavitt, M.N. Robertson, D.V. Mehrotra, E. Quirk, Safety and immunogenicity of a replication-incompetent adenovirus type 5 HIV-1 clade B gag/pol/nef vaccine in healthy adults, Clin. Infect. Dis. 46 (2008) 1769–1781.

doi:10.1093/brain/awt183 Brain 2013: 136; 2876–2887 | 2876

BRAIN
A JOURNAL OF NEUROLOGY

Positive feedback loop via astrocytes causes chronic inflammation in virus-associated myelopathy

Hitoshi Ando,[1] Tomoo Sato,[1] Utano Tomaru,[2] Mari Yoshida,[3] Atae Utsunomiya,[4] Junji Yamauchi,[1] Natsumi Araya,[1] Naoko Yagishita,[1] Ariella Coler-Reilly,[1] Yukiko Shimizu,[1] Kazuo Yudoh,[5] Yasuhiro Hasegawa,[6] Kusuki Nishioka,[7] Toshihiro Nakajima,[7] Steven Jacobson[8] and Yoshihisa Yamano[1]

1 Department of Rare Diseases Research, Institute of Medical Science, St. Marianna University School of Medicine, Kanagawa, Japan
2 Department of Pathology, Hokkaido University Graduate School of Medicine, Sapporo, Japan
3 Institute for Medical Science of Ageing, Aichi Medical University, Aichi, Japan
4 Department of Haematology, Imamura Bun-in Hospital, Kagoshima, Japan
5 Institute of Medical Science, St. Marianna University School of Medicine, Kanagawa, Japan
6 Department of Neurology, St. Marianna University School of Medicine, Kanagawa, Japan
7 Institute of Medical Science, Tokyo Medical University, Tokyo, Japan
8 Viral Immunology Section, Neuroimmunology Branch, National Institutes of Health, Bethesda, MD, USA

Correspondence to: Yoshihisa Yamano, MD, PhD
Department of Rare Diseases Research,
Institute of Medical Science,
St. Marianna University School of Medicine,
2-16-1, Sugao, Miyamae-ku,
Kawasaki 216-8512,
Japan
E-mail: yyamano@marianna-u.ac.jp

Human T-lymphotropic virus type 1-associated myelopathy/tropical spastic paraparesis (HAM/TSP) is a rare neurodegenerative disease characterized by chronic inflammation in the spinal cord. We hypothesized that a positive feedback loop driven by chemokines may be responsible for the chronic inflammation in HAM/TSP. We aimed to determine the identity of these chemokines, where they are produced, and how they drive chronic inflammation in HAM/TSP. We found that patients with HAM/TSP have extraordinarily high levels of the chemokine CXCL10 (also known as IP-10) and an abundance of cells expressing the CXCL10-binding receptor CXCR3 in the cerebrospinal fluid. Histological analysis revealed that astrocytes are the main producers of CXCL10 in the spinal cords of patients with HAM/TSP. Co-culture of human astrocytoma cells with $CD4^+$ T cells from patients with HAM/TSP revealed that astrocytes produce CXCL10 in response to IFN-γ secreted by $CD4^+$ T cells. Chemotaxis assays results suggest that CXCL10 induces migration of peripheral blood mononuclear cells to the central nervous system and that anti-CXCL10 neutralizing antibody can disrupt this migration. In short, we inferred that human T-lymphotropic virus type 1-infected cells in the central nervous system produce IFN-γ that induces astrocytes to secrete CXCL10, which recruits more infected cells to the area via CXCR3, constituting a T helper type 1-centric positive feedback loop that results in chronic inflammation.

Keywords: HTLV-1; HAM/TSP; CXCL10; CXCR3; astrocyte
Abbreviation: HAM/TSP = human T-lymphotropic virus type 1-associated myelopathy/tropical spastic paraparesis

Received February 18, 2013. Revised May 3, 2013. Accepted May 26, 2013. Advance Access publication July 26, 2013

Introduction

The rise of chronic inflammatory disorders has prompted researchers to reconsider the classical concept of inflammation, which dates back to ancient Roman times when inflammation was first defined as redness, swelling, heat and pain in response to injury or infection. In general, inflammation is an adaptive immune response to tissue malfunction that ideally neutralizes the source of the disturbance and restores tissue homeostasis. Paradoxically, a prolonged state of inflammation has been implicated in the pathogenesis of various diseases characterized by the loss of homeostasis, such as autoimmune diseases, cancers and neurodegenerative diseases (Libby, 2002; Mantovani *et al.*, 2008; Medzhitov, 2008, 2010). To produce effective therapies for these debilitating disorders, we must first elucidate the mechanisms by which this maladaptive chronic inflammatory state develops.

Although there are many chronic inflammatory disorders for which the initiating trigger is ill-defined or unknown, human T-lymphotropic virus type 1 (HTLV-1)-associated myelopathy/tropical spastic paraparesis (HAM/TSP) is a rare neurodegenerative chronic inflammatory disease clearly caused by HTLV-1 retroviral infection (Gessain *et al.*, 1985; Osame *et al.*, 1986). In other words, the HTLV-1-infected cells in patients with HAM/TSP represent a useful starting point from which to investigate the origins of chronic inflammation.

HTLV-1 infects 10–20 million people worldwide, some of whom develop serious conditions such as adult T cell leukaemia (Hinuma *et al.*, 1981) and up to 2–3% of whom develop the debilitating inflammation in the spinal cord that characterizes HAM/TSP (Gessain *et al.*, 1985; Osame *et al.*, 1986). Evidence has accumulated to support the theory that infected $CD4^+$ T cells (as opposed to infected neuronal cells or non-infected peripheral blood mononuclear cells) are primarily responsible for this transition to the HAM/TSP disease state: HTLV-1 primarily infects $CD4^+$ T cells (Richardson *et al.*, 1990); levels of infected $CD4^+$ T cells circulating in the blood of patients with HAM/TSP are higher than those in the blood of asymptomatic carriers (Nagai *et al.*, 1998; Yamano *et al.*, 2002), the levels in the CSF surrounding the spinal cord are higher still (Nagai *et al.*, 2001*a*); and these infected $CD4^+$ T cells have also been detected in the spinal cord lesions themselves (Moritoyo *et al.*, 1996; Matsuoka *et al.*, 1998). There are many cell types capable of producing an inflammatory response upon contact with viral antigens, and it is true that the cases where these antigen-specific cells are most abundant are indeed in patients with HAM/TSP, but there is a large range of overlap in which patients with HAM/TSP and asymptomatic carriers have the same amount of antigen-specific cells in their peripheral blood mononuclear cells (Jacobson *et al.*, 1990; Jeffery *et al.*, 1999; Kubota *et al.*, 2000; Yamano *et al.*, 2002). Therefore, we hypothesized that their presence may not be the key factor that determines a patient's fate to experience the disease or not, and that perhaps there might be another cell type responsible for initiating the chronic inflammation in HAM/TSP through a more unique pathway. Research shows that infected $CD4^+$ T cells are indeed capable of migrating across the blood–brain barrier into the CNS (Furuya *et al.*, 1997) and secreting proinflammatory cytokines such as interferon-gamma (IFN-γ) (Hanon *et al.*, 2001; Yamano *et al.*, 2005, 2009). We guessed that these cells might even be capable of producing IFN-γ spontaneously due only to intracellular activation of transcription factors by the invading HTLV-1 virus, which has been shown to be capable of such potent effects (Waldmann, 2006).

Studies have indicated that among the $CD4^+$ T cell subtypes, immune responses by $CD4^+$ T helper type 1 (Th1)-like cells may be dominant in patients with HAM/TSP (Goon *et al.*, 2002; Narikawa *et al.*, 2005), leading to the theory that the Th1 axis should be the primary focus in the study of HAM/TSP. These Th1 cells express both the CC chemokine receptor type 5 (CCR5) and CXC motif receptor 3 (CXCR3), which respond to the presence of CC motif ligand (CCL) 3, 4 and 5 and CXC motif ligand (CXCL) 9, 10 and 11, respectively. These ligands are chemokines, a subclass of cytokines that stimulate directed chemotaxis in responsive cells, and it is known that chemokine receptor–ligand interactions play an important role in recruiting immune cells to inflammatory sites (Luster, 1998; Qin *et al.*, 1998). Of particular interest are the CXCR3 agonists, which are regulated by the aforementioned proinflammatory cytokine IFN-γ and carry this relationship in the alternative nomenclature: monokine induced by gamma interferon (MIG/CXCL9), IFN-γ-inducible protein 10 (IP-10/CXCL10), and interferon-inducible T cell alpha chemoattractant (I-TAC/CXCL11) (Proost *et al.*, 2001, 2003). We and others have shown that CCL5, CXCL9, and especially CXCL10, are elevated in the CSF of patients with HAM/TSP (Teixeira *et al.*, 2004; Narikawa *et al.*, 2005; Tanaka *et al.*, 2008; Sato, in press).

We hypothesized that these chemokines play a key role in the pathogenesis of HAM/TSP by recruiting more cells infected with HTLV-1 to the inflammation site and potentially initiating a positive feedback loop. We first compared the levels of several chemokines in the serum and CSF of patients with HAM/TSP and asymptomatic carriers and found that CXCL10 was the most closely associated with known features of HAM/TSP pathogenesis, namely increased CSF cell count. We then analysed samples of peripheral blood mononuclear cells and CSF cells along with images of the spinal cord tissue to demonstrate that $CD4^+$ cells expressing CXCL10-binding CXCR3, namely cells of the Th1 subtype, are indeed infected with HTLV-1, do migrate across the blood–brain barrier into the CNS, and do produce IFN-γ in patients with HAM/TSP. We demonstrated that this IFN-γ production can occur in the absence of external stimuli. Immunohistochemical analysis of the spinal cord tissue not only confirmed that CXCL10 production is elevated in patients with HAM/TSP but also revealed that astrocytes may be the main producers of CXCL10 in the spinal cord. We used novel techniques to demonstrate that these astrocytes likely represent the missing piece of the puzzle in the positive feedback loop: infected $CD4^+$ T cells produce IFN-γ, which stimulates astrocytes to produce CXCL10, which recruits more $CD4^+CXCR3^+$ Th1 cells to the CNS. Finally, chemotaxis assays were used to compare the inhibitory potentials of anti-CXCL10 and anti-CXCR3 neutralizing antibodies on this positive feedback loop as the first step toward the development of an effective therapy.

Materials and methods

Patient selection and sample preparation

Written informed consent was obtained from all patients before the study, which was reviewed and approved by the Institutional Ethics Committee (St. Marianna University) and conducted in compliance with the tenets of the Declaration of Helsinki. The study included 26 HTLV-1 non-infected healthy donors (14 females and 12 males; mean age, 49 years), 29 asymptomatic carriers (21 females and eight males; mean age, 50 years), 17 patients with adult T cell leukaemia with no history of chemotherapy (eight females and nine males; mean age, 68 years), and 58 patients with HAM/TSP (47 females and 12 males; mean age, 62 years). Diagnosis of adult T cell leukaemia was based on the criteria established by Shimoyama (1991). HTLV-1 seropositivity was determined by a particle agglutination assay (Serodia-HTLV-1) and confirmed by western blot (SRL Inc.). HAM/TSP was diagnosed according to WHO guidelines (Osame, 1990).

Samples of peripheral blood mononuclear cells were prepared using density gradient centrifugation (Pancoll; PAN-Biotech) and viably cryopreserved in liquid nitrogen with freezing medium (Cell Banker 1; Mitsubishi Chemical Medience Corporation). Plasma and serum samples were obtained from 16 healthy donors, 26 asymptomatic carriers, 30 patients with HAM/TSP and 14 patients with adult T cell leukaemia (six smouldering type and eight chronic type). Multiple serum and CSF samples were taken within a 1-h window for each of 32 patients with HAM/TSP. A Fuchs–Rosenthal chamber (Hausser Scientific Company) was used for CSF cell counts, after which the cells were isolated by centrifugation and cryopreserved in the aforementioned freezing medium. A medulla oblongata tissue sample from one patient with HAM/TSP as well as thoracic spinal cord tissues from four patients with HAM/TSP and six control individuals with no spinal cord lesions (numbered controls 1–6; one female and five males; mean age, 67 years) were obtained post-mortem, fixed in 10% formalin, and embedded in paraffin. Clinical characteristics of the patients with HAM/TSP who underwent post-mortem examination are shown in Supplementary Table 1.

Cell culture

Before culture, peripheral blood mononuclear cells from patients with HAM/TSP, asymptomatic carriers and healthy donors were sorted using MACS beads (Miltenyi Biotec) according to the manufacturer's instructions; $CD4^+$ T cells and $CD8^+$ T cells were separated negatively, and $CD14^+$ cells were separated positively, and the purity of all cell populations exceeded 95%. The isolated cells were seeded at 1×10^5 cells/200 μl/well in 96-well round-bottom plates in RPMI 1640 medium (Wako Pure Chemical Industries Ltd.) supplemented with 10% heat-inactivated human serum (Wako Pure Chemical Industries Ltd.), and 1% penicillin/streptomycin antibiotic solution (Wako Pure Chemical Industries Ltd.) without any stimuli. The culture supernatants were collected after incubating at 37°C for 24, 48 and 72 h in 5% CO_2.

U251 human astrocytoma cells were cultured in Dulbecco's minimal essential medium (Wako Pure Chemical Industries Ltd.) supplemented with 10% heat-inactivated foetal bovine serum (Gibco-Invitrogen) and 1% penicillin/streptomycin. In total, 2×10^4 U251 cells were then co-cultured in 48-well flat-bottom plates at 37°C for 48 h in 5% CO_2 with 0, 2×10^2, 2×10^3 or 2×10^4 $CD4^+$ T cells isolated from peripheral blood mononuclear cells of patients with HAM/TSP or healthy donors using MACS beads. A control group of 2×10^4 $CD4^+$ T cells was single-cultured under the same conditions. The U251 cells were also cultured with and without 1 ng/ml recombinant human IFN-γ (285-IF, R&D Systems). After culture for 48 h, $CD4^+$ T cells were removed by washing with PBS and the U251 cells were then cultured for an additional 24 h before collecting the culture supernatants.

For the experiment investigating the inhibitory potential of neutralizing antibodies, 2×10^4 $CD4^+$ T cells isolated from peripheral blood mononuclear cells of patients with HAM/TSP using MACS beads were cultured in 96-well round-bottom plates for 72 h under the same conditions, and the culture supernatant was collected after centrifugation. Then, in this supernatant, 2×10^4 U251 cells were cultured in 48-well flat-bottom plates with 10 μg/ml monoclonal neutralization antibodies: anti-IFN-γ antibody (MAB285, R&D Systems), anti-tumour necrosis factor (TNF)-α antibody (MAB610, R&D Systems), or isotype control antibody (MAB002 and MAB003, R&D Systems). The U251 cells were cultured for additional 24 h before collecting the culture supernatants for assay.

Measurement of chemokines, IFN-γ, IL-17A and sIL-2 receptor

The concentrations of four chemokines (CCL4, CCL5, CXCL9 and CXCL10) in the serum and CSF samples and levels of CXCL10, IFN-γ and IL-17A in the culture supernatants were measured with a cytometric bead array kit (BD Biosciences) using a FACSCalibur flow cytometer (BD Biosciences) according to the manufacturer's instructions. It should be noted that the cytometric bead array kit measures the total concentrations of all chemokine isoforms irrespective of aminoterminal variation (Proost *et al.*, 2001, 2003). The sIL-2R in the serum was measured using an ELISA (Cell-free N IL-2R, Kyowa Medex).

Flow cytometric analysis

Peripheral blood mononuclear cells and CSF cells, which were obtained on the same day, were immunostained with various combinations of the following fluorescence-conjugated antibodies: anti-CD3 (UCHT1), anti-CD4 (OKT4), anti-CD8 (RPA-T8), anti-CD19 (HIB19), anti-CD14 (61D3) (all from eBioscience), and anti-CXCR3 (1C6; BD Biosciences). The cells were stained with a saturating concentration of antibody in the dark (4°C, 30 min) and washed twice before analysis using FACSCalibur (BD Biosciences). Data were processed using FlowJo software (TreeStar). For cell sorting, JSAN (Bay Bioscience,) was used, and the purity exceeded 95%.

Real-time polymerase chain reaction

The HTLV-1 proviral DNA load was measured using ABI Prism 7500 SDS (Applied Biosystems) as described previously (Yamano *et al.*, 2002). In brief, DNA was extracted and 100 ng samples were analysed per well. The proviral DNA load was calculated using the following formula: copy number of HTLV-1 (*pX*) per 100 cells = (copy number of *pX*) / (copy number of β-actin / 2) × 100.

Tissue staining

Formalin-fixed thoracic spinal cord and medulla oblongata tissue sections were deparaffinized in xylene and rehydrated in a series of

graded alcohols and distilled water. The antigenicity of the tissue sections was recovered using a standard microwave heating technique. For immunohistochemistry, the slides were incubated with anti-CXCL10/IP-10 antibody, followed by detection with streptavidin–biotin–horseradish peroxidase and diaminobenzidine (DakoCytomation Japan Co. Ltd.). The $CXCL10^+$ cells in the spinal cord were also counted under the microscope; the data show the mean number of cells in three random 1-mm^2 fields per sample. Haematoxylin and eosin staining was conducted to detect inflammatory cells that had invaded the tissue samples. For immunofluorescence (thoracic spinal cord sections only), the slides were incubated in phosphate-buffered saline with 10% goat serum for 1 h at room temperature, in anti-CXCR3 antibody (Abcam), anti-CXCL10/IP-10 antibody (Santa Cruz Biotechnology), and anti-glial fibrillary acidic protein (GFAP) antibody (DakoCytomation Japan Co. Ltd) overnight at 4°C, labelled with Alexa Fluor® 488 or Alexa Fluor® 594 conjugated secondary antibody (Invitrogen), and examined under a fluorescence microscope (Nikon eclipse E600 with fluorescence filter Nikon F-FL; Nikon Instech) with rabbit or mouse immunoglobulin G (IgG) as the negative control.

Chemotaxis assay

Peripheral blood mononuclear cells from patients with HAM/TSP were washed and then suspended (at 1×10^7 cells/ml) in 37°C serum-free RPMI 1640 medium containing 1 mg/ml bovine serum albumin (Wako Pure Chemical Industries, Ltd.), hereafter 'chemotaxis medium'. The lower wells of a 96-well chemotaxis chamber (MBA96; Neuroprobe) were filled with chemotaxis medium containing 0.25 μg/ml recombinant human CXCL10 protein (266-IP; R&D Systems). For the negative control, the lower wells were filled with only the chemotaxis medium. For chemotaxis assays using neutralizing monoclonal antibodies, peripheral blood mononuclear cells were pretreated (room temperature, 30 min) with 10 μg/ml of anti-CXCL10 antibody (MAB266; R&D Systems), 10 μg/ml of anti-CXCR3 antibody (MAB160; R&D Systems), or 10 μg/ml of isotype control antibody (MAB002; R&D Systems). A polyvinylpyrrolidone-free micropore polycarbonate filter (PFD5; Neuroprobe) with 5-μm pores was placed over the lower chamber. The upper wells were filled with 1×10^6 peripheral blood mononuclear cells in 100 μl of chemotaxis medium. The chamber was incubated for 120 min at 37°C in a humidified 5% CO_2 atmosphere. After incubation, the fluid in the lower chambers was collected and cell counts were determined using FACSCalibur. To compare results across all chemotaxis assays, a chemotactic index was calculated using the following formula (Nie *et al.*, 2009):

$$\text{Chemotactic index} = (\text{number of migrated cells in a test sample well})/(\text{number of migrated cells in a negative control well})$$

To determine the inhibitory effect of neutralizing antibodies, an inhibitory efficiency scale was calculated using the following formula:

$$\text{Inhibitory efficiency (\% inhibition)} = \{[(\text{chemotactic index of isotype control}) - 1] - [(\text{chemotactic index of neutralizing antibody}) - 1]\}/[(\text{chemotactic index of isotype control}) - 1] \times 100$$

Proliferation assay

The migrated cells in the lower chamber after the chemotaxis assay were collected and washed with RPMI 1640 medium supplemented with 5% foetal bovine serum and 1% penicillin/streptomycin. Those cells were then plated on 96-well round-bottom plates and cultured in the same medium without any mitogenic stimuli in 5% CO_2 at 37°C. Cell proliferation was measured using a ^{3}H-thymidine incorporation assay as described previously (Yamano *et al.*, 2009).

Statistical analysis

Correlation analysis was assessed using Spearman's rank test. The paired *t*-test was used for within-group comparisons, and the *t*-test or the Mann–Whitney U-test was used for comparisons between groups. One-way ANOVA was used for multiple comparisons followed by Tukey's test. The Friedman test was used for paired multiple comparisons, followed by the Dunn test. Statistical analyses and graphs were performed using Graphpad Prism 5 and Prism statistics (GraphPad Software, Inc), and statistical significance was set at $P < 0.05$.

Results

Significantly higher levels of cerebrospinal fluid CXCL10 compared with serum CXCL10 in patients with HAM/TSP

To determine whether the aforementioned chemokines were involved in the migration of cells to the CNS, we first compared the levels of these chemokines with CSF cell counts in patients with HAM/TSP ($n = 29$). CSF cell counts significantly correlated with levels of CXCL10 and CXCL9 but not with those of CCL5 or CCL4, the negative control (Fig. 1A). In addition, the correlation was clearly stronger with CXCL10 than with CXCL9. Following this, we compared the CSF and serum levels of these chemokines. Interestingly, only CXCL10 levels were higher in the CSF than the serum, although serum CXCL10 levels were also high to some extent (Fig. 1B, $P < 0.0001$). Next, to investigate whether these high CXCL10 levels were a HAM/TSP-specific phenomenon within HTLV-1-associated disorders, we tested for a correlation between CXCL10 and soluble interleukin-2 receptor (sIL-2R), a marker for adult T cell leukaemia (Yasuda *et al.*, 1988). As expected, serum sIL-2R levels were the highest in patients with adult T cell leukaemia. By contrast, plasma CXCL10 levels were significantly higher in patients with HAM/TSP than in those with adult T cell leukaemia, asymptomatic carriers or healthy donors (Supplementary Fig. 1A). This higher concentration of plasma CXCL10 in patients with HAM/TSP was observed even when compared to asymptomatic carriers with equivalently high proviral loads (Supplementary Fig. 1B).

Existence of abundant $CXCR3^+$ cells in the spinal cords of patients with HAM/TSP

Because CXCL10 is a ligand of CXCR3, we investigated the possibility of CXCL10 recruiting proinflammatory $CXCR3^+$ cells into the CSF by measuring the presence of $CXCR3^+$ cells in the CSF and spinal cord lesions of patients with HAM/TSP (Fig. 2A–C). Flow cytometric analysis revealed that the average percentage of

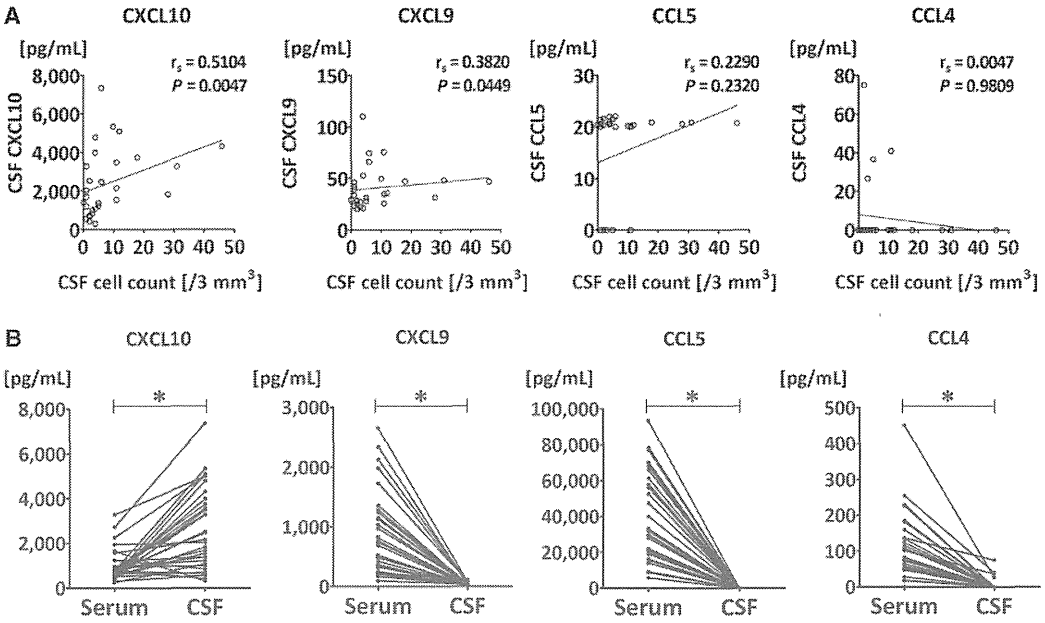

Figure 1 CXCL10 levels in CSF of patients with HAM/TSP were correlated with CSF cell counts and were significantly higher than those in serum of patients with HAM/TSP. (**A**) Correlation analysis between CSF levels of four chemokines (CXCL10, CXCL9, CCL5 and CCL4) and CSF cell counts in patients with HAM/TSP ($n = 29$). Statistical analysis was performed using Spearman's rank test. The linear regression line is indicated by a straight line in each graph. (**B**) Comparison of concentrations of four chemokines (CXCL10, CXCL9, CCL5, and CCL4) in CSF and serum samples obtained from patients with HAM/TSP such that all samples from a given patient were taken within a 1-h window of the first sample taken from that patient ($n = 32$). *$P < 0.0001$ by the paired t-test.

CXCR3$^+$ cells among CSF cells was 92.4 ± 7.0%, whereas the average percentage of CXCR3$^+$ cells among peripheral blood mononuclear cells was 9.9 ± 8.2% ($P < 0.0001$, Fig. 2B). Immunofluorescence staining revealed abundant CXCR3$^+$ cell infiltrate around small vessels in the leptomeninges of spinal cord lesions in patients with HAM/TSP (Fig. 2C). We examined the types of CXCR3$^+$ cells in the CSF using flow cytometry and found that CSF CXCR3$^+$ cells mainly consist of CD3$^+$ cells (>90%) and small populations of CD14$^+$ and CD19$^+$ cells (Fig. 2D, left). Uniquely, the percentage of CXCR3$^+$ cells was extremely high in all CSF cell populations under study, especially CD4$^+$ (94.33 ± 2.95%), CD8$^+$ (98.64 ± 1.05%), and even CD14$^+$ (84.97 ± 18.49%) and CD19$^+$ (76.38 ± 17.35%) cells (Supplementary Fig. 2). Our data show that the ratio of CD4$^+$ to CD8$^+$ cells in the CSF was ~1:1 in patients with HAM/TSP (Fig. 2D, right). In both these cell populations, the rate of CXCR3 positivity was higher in CSF cells than in peripheral blood mononuclear cells (Supplementary Fig. 2). The percentage of CXCR3$^+$ cells in peripheral blood mononuclear cells of patients with HAM/TSP was lower than those in peripheral blood mononuclear cells of asymptomatic carriers as well as healthy donors; however, there were no significant differences between patients with adult T cell leukaemia and patients with HAM/TSP (Supplementary Fig. 3A). This lower percentage of CXCR3$^+$ cells in patients with HAM/TSP was observed even when compared with asymptomatic carriers with equivalently high proviral loads (Supplementary Fig. 3B). Finally, to support our hypothesis that HTLV-1-infected T cells (the majority of which are known to be CD4$^+$) migrate from the circulating blood to the spinal cord tissue through CXCL10–CXCR3 interaction, we confirmed that there does exist a subset of peripheral CD4$^+$CXCR3$^+$ T cells infected with HTLV-1 (Fig. 2E).

Numerous CXCL10-producing cells in inflamed spinal cords of patients with HAM/TSP

To quantitatively compare the level of expression of CXCL10, we microscopically counted the number of CXCL10$^+$ cells in the spinal cord tissue and found a larger number of CXCL10$^+$ cells in the spinal cord lesions of patients with HAM/TSP than in control patients (Fig. 3A, $P = 0.0095$). In addition, we compared tissue sections from the thoracic spinal cord (a region of high inflammation) and the medulla oblongata (comparatively very low inflammation) from a single patient with HAM/TSP, and we observed a much larger CXCL10 presence in the thoracic spinal cord region (Supplementary Fig. 4).

Astrocytes as the main producers of CXCL10 in the spinal cords of patients with HAM/TSP

To identify which cell populations are the main CXCL10 producers, we immunostained thoracic spinal cord tissues from patients with

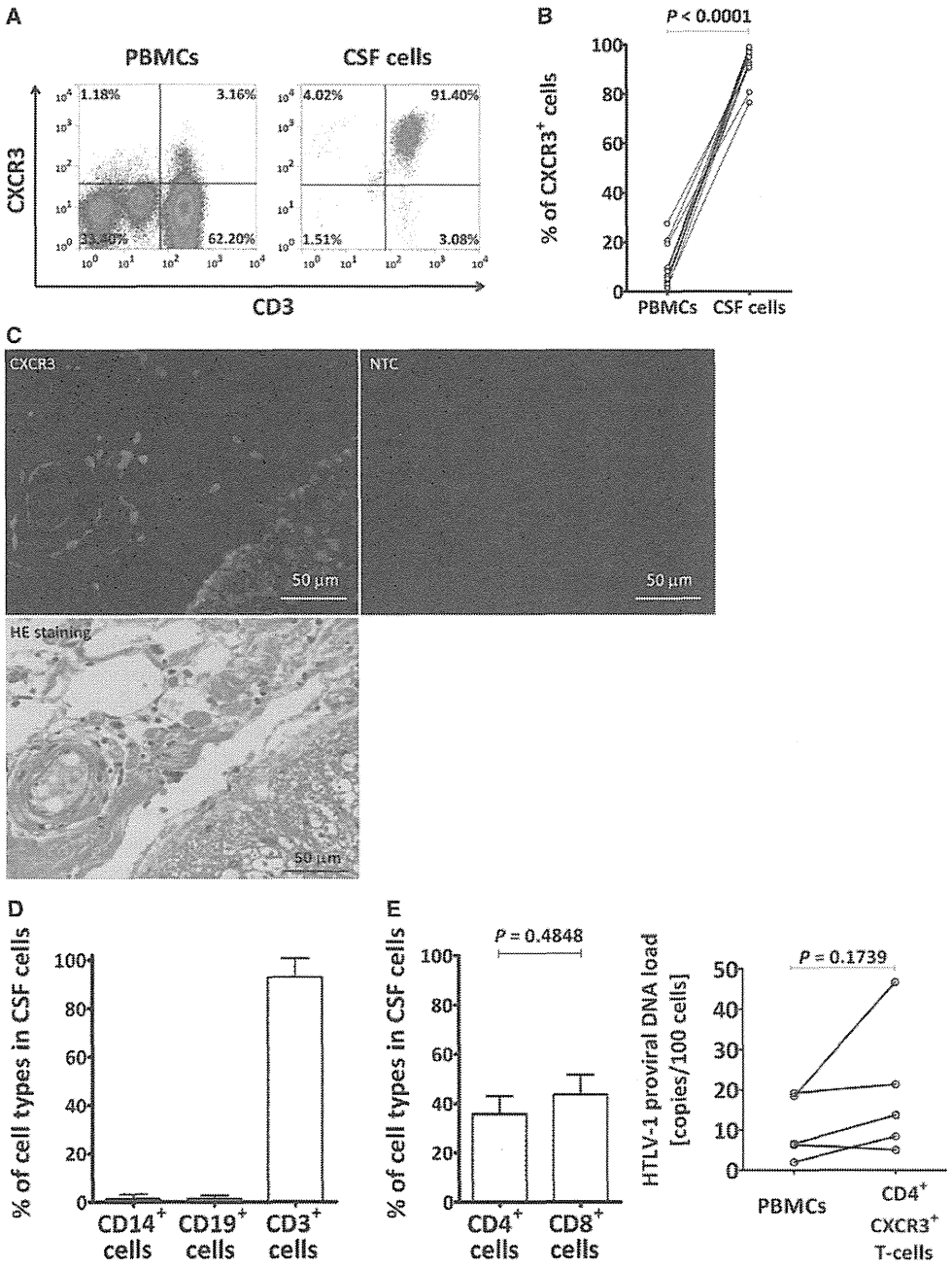

Figure 2 Abundant CXCR3$^+$ cells in the CSF and spinal cord tissue of patients with HAM/TSP. (**A**) Representative dot plots of CD3 and CXCR3 expression in peripheral blood mononuclear cells (PBMCs, *left*) and CSF cells (*right*) from a patient with HAM/TSP measured using flow cytometry. (**B**) Comparison of the percentages of CXCR3$^+$ cells in peripheral blood mononuclear cells and CSF cells, samples of which were obtained from 12 patients with HAM/TSP such that all samples from a given patient were taken within a 1-h window of the first sample taken from that patient. Statistical analysis was performed using the paired *t*-test. See also Supplementary Fig. 2. (**C**) Representative images of immunofluorescent detection of CXCR3, shown in green (*upper* panels), and haematoxylin-eosin (HE) staining for inflammatory cells, shown in blue (*lower* panel), in the thoracic spinal cords of patients with HAM/TSP. Rabbit IgG antibody used as the negative control (NTC). (**D**) *Left*: Percentages of CD3$^+$, CD19$^+$, and CD14$^+$ cells in CSF cells derived from patients with HAM/TSP ($n = 6$). *Right*: Percentages of CD4$^+$ cells and CD8$^+$ cells. Statistical analysis was performed using the Mann–Whitney U-test. Error bars represent the mean ± SD. (**E**) The HTLV-1 proviral DNA loads of CD4$^+$CXCR3$^+$ T cells with peripheral blood mononuclear cells as the control. This result confirms the non-negligible existence of HTLV-1-infected CD4$^+$CXCR3$^+$ T cells, which may migrate to the CNS. Cells are from patients with HAM/TSP ($n = 5$). Statistical analysis was performed using the paired *t*-test.

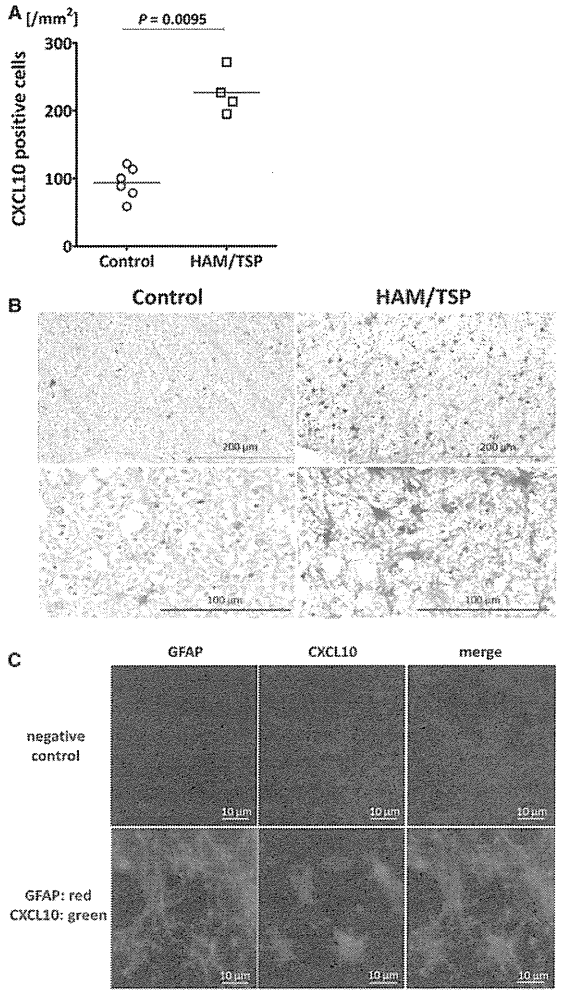

Figure 3 Astrocytes are the major CXCL10-producing cells in the spinal cords of patients with HAM/TSP. (**A**) Quantitative histological analysis (control: $n = 6$, HAM/TSP: $n = 4$). The numbers of CXCL10$^+$ cells in the spinal cord sections were counted under a microscope. The data represent the mean number of CXCL10$^+$ cells in three random fields of 1 mm^2 per sample. Horizontal bars represent the mean. Statistical analysis was performed using the Mann–Whitney U-test. (**B**) Representative immunohistochemistical images of CXCL10 in the thoracic spinal cord tissues from control individuals ($n = 6$) and patients with HAM/TSP ($n = 4$). CXCL10-positive cells are brown. *Upper* panel: low magnification; *Lower* panel: high magnification. (**C**) Representative immunofluorescent images of GFAP (red), a marker for astrocytes, and CXCL10 (green) in the thoracic spinal cord tissues from a control individual and a patient with HAM/TSP patient. Similar results were observed in images of spinal cord tissues obtained from two other patients with HAM/TSP.

HAM/TSP ($n = 4$) and control individuals ($n = 6$). CXCL10-positive staining was mainly observed in star-shaped cells with extensive and radiating cytoplasmic processes, indicating that CXCL10 is expressed in activated astrocytes in the thoracic spinal cord of patients with HAM/TSP (Fig. 3B). We also used immunofluorescence to confirm that CXCL10 is mainly expressed in astrocytes (GFAP$^+$ cells) (Fig. 3C).

Co-culture with CD4$^+$ T cells from patients with HAM/TSP enhances CXCL10 production in U251 human astrocytoma cells

CXCL10, also known as an IFN-γ-inducible protein 10, is mainly produced in response to IFN-γ stimulation (Muller *et al.*, 2010). We used this fact to investigate the events leading to CXCL10 production by astrocytes in the spinal cords of patients with HAM/TSP. First, we compared the capacities of several purified cell populations within peripheral blood mononuclear cells to produce IFN-γ spontaneously, i.e. without any stimulation. We found that CD4$^+$ T cells exhibited the highest production of IFN-γ among peripheral blood mononuclear cells isolated from patients with HAM/TSP, and CD4$^+$ T cells from patients with HAM/TSP produced more IFN-γ than those from asymptomatic carriers (Fig. 4A and B left). No peripheral blood mononuclear cells isolated from healthy donors displayed any detectable level of IFN-γ production (data not shown). Interestingly, CD4$^+$ T cells from patients with HAM/TSP did not produce IL-17A, a proinflammatory cytokine known to play a key role in the pathogenic inflammatory response that characterizes multiple sclerosis (Fig. 4B, right) (Matusevicius *et al.*, 1999). Next, we used a co-culture system to confirm that CD4$^+$ T cells induce astrocytes to produce CXCL10 by releasing IFN-γ. CD4$^+$ T cells from patients with HAM/TSP induced CXCL10 production in U251 astrocytoma cells in a cell number-dependent manner (Fig. 4C), whereas CD4$^+$ T cells from healthy donors did not induce CXCL10 production (data not shown). Importantly, in the presence of anti-IFN-γ neutralizing antibodies, the supernatant from HAM/TSP patient CD4$^+$ T cell cultures stimulated significantly less CXCL10 production in U251 cells (Fig. 4D).

Chemotaxis of peripheral blood mononuclear cells from patients with HAM/TSP due to CXCL10 and inhibition of chemotaxis by anti-CXCL10 neutralizing antibodies

To investigate the potential role of CXCL10 or CXCR3 as a therapeutic target for inhibiting the migration of proinflammatory cells into the CNS, we assessed whether neutralizing antibodies against CXCL10 or CXCR3 could inhibit the migration of peripheral blood mononuclear cells in patients with HAM/TSP through the use of an *in vitro* chemotaxis assay system. Human CXCL10 increased the chemotactic activity of peripheral blood mononuclear cells from patients with HAM/TSP by ~1.7-fold (Fig. 5A). Compared with isotype control monoclonal antibodies, the chemotactic activity due to CXCL10 was inhibited by anti-CXCL10 neutralizing antibodies (Fig. 5A; 65.9% inhibition, $P < 0.01$) but not by anti-CXCR3 antibodies (Fig. 5A; 9.2% inhibition, $P > 0.05$: not

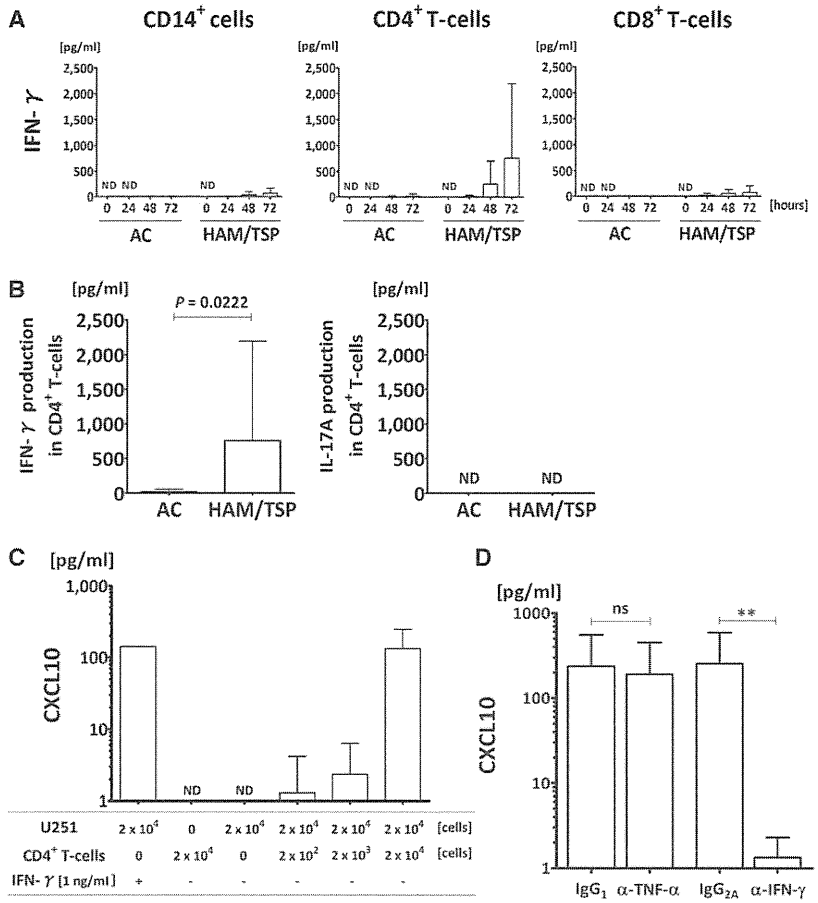

Figure 4 Co-culturing with CD4$^+$ T cells from patients with HAM/TSP increases CXCL10 production in a U251 human astrocytoma cell line. (**A**) Concentration of IFN-γ in supernatants of cultured CD4$^+$, CD8$^+$, or CD14$^+$ cells in peripheral blood mononuclear cells (PBMCs) from patients with HAM/TSP ($n = 6$) compared with that in peripheral blood mononuclear cells from asymptomatic carriers (AC, $n = 5$). These cells were cultured without any stimuli for 24, 48 and 72 h. ND = not detected. (**B**) Concentrations of IFN-γ (*left*) and IL-17A (*right*) in culture supernatants of cultured CD4$^+$ T cells for 72 h from patients with HAM/TSP compared with the concentrations in those from asymptomatic carriers. Patients with HAM/TSP: $n = 6$, asymptomatic carrier: $n = 5$. ND = not detected. Statistical analyses were performed using the Mann–Whitney U-test. (**C**) Concentration of CXCL10 produced by U251, a human astrocytoma cell line, co-cultured with CD4$^+$ T cells from patients with HAM/TSP ($n = 5$). ND = not detected. (**D**) Concentration of CXCL10 produced by U251 stimulated by the supernatant of cultured CD4$^+$ T cells of patients with HAM/TSP ($n = 5$) in the presence of neutralizing antibodies against IFN-γ and TNF-α, and isotype control antibodies for each. NS = not significant. $^{**}P < 0.01$. Error bars represent the mean ± SD.

significant). Next, we investigated whether or not this decreased migration would also be reflected in the absolute number of HTLV-1-infected cells among migrated cells. Chemotaxis assays revealed that the addition of human CXCL10 (0.25 μg/ml) increased the absolute number of HTLV-1-infected cells by ~2.1-fold (Fig. 5B) compared with isotype control monoclonal antibodies, and that this increase was largely inhibited by anti-CXCL10 neutralizing antibodies (Fig. 5B; 101.1% inhibition, $P < 0.01$) but only slightly by anti-CXCR3 antibodies (Fig. 5B; 65.7% inhibition, $P > 0.05$: not significant). Finally, we evaluated the degree to which the migrated cells were proliferating spontaneously, where spontaneous proliferation is defined as proliferation in the absence of exogenous antigens or stimulants (Itoyama *et al.*, 1988; Ijichi *et al.*, 1989). This is important because the level of spontaneous proliferation of peripheral blood mononuclear cells in patients with HAM/TSP is believed to reflect the cell proliferation that occurs in the CNS (Itoyama *et al.*, 1988; Ijichi *et al.*, 1989). Significantly less ^{3}H-thymidine uptake, an assay for cell proliferation, was detected in the lower chemotaxis assay chamber following administration of anti-CXCL10 antibody than isotype control antibodies (Fig. 5C; 33.8% inhibition, $P < 0.05$).

Discussion

Previous studies of HAM/TSP pathogenesis have revealed that chronic inflammation occurs in the spinal cords of patients with HAM/TSP (Saito and Bangham, 2012; Yamano and Sato, 2012);

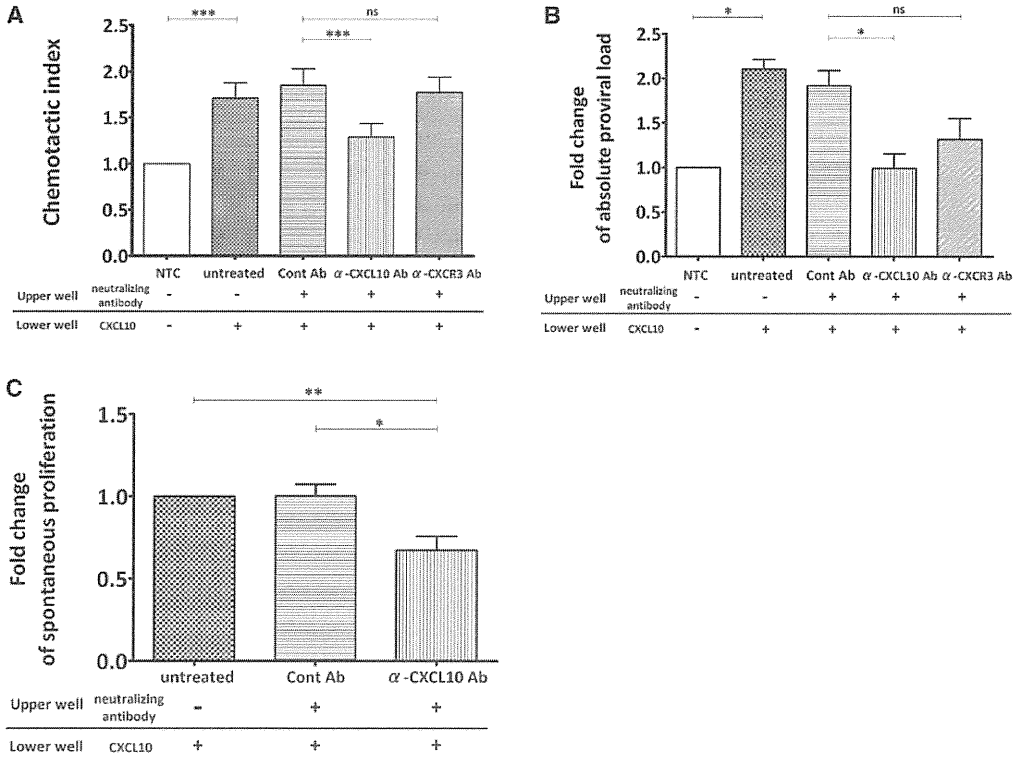

Figure 5 Chemotaxis of peripheral blood mononuclear cells due to CXCL10 and inhibition of chemotaxis by anti-CXCL10 neutralizing antibody in cells from patients with HAM/TSP. (**A**) The migration-inducing effect of CXCL10 and the inhibitory effect of neutralizing antibody against CXCL10 versus its receptor, CXCR3. Peripheral blood mononuclear cells from patients with HAM/TSP ($n = 21$) migrated into the lower well in response to CXCL10, and treatment with anti-CXCL10 antibody significantly reduced the migration of peripheral blood mononuclear cells, as compared to anti-CXCR3 antibody and control antibody. (**B**) The inhibition of cell migration led to an overall decrease in migrated cells including HTLV-1-infected cells, effectively decreasing the absolute proviral load. Peripheral blood mononuclear cells used were collected from patients with HAM/TSP; $n = 4$. (**C**) The inhibition of cell migration led to an overall decrease in migrated cells which also means less spontaneous proliferation. Peripheral blood mononuclear cells used were collected from patients with HAM/TSP; $n = 7$. Error bars represent the mean ± SD. Statistical analyses were performed using the Friedman test followed by the Dunn test for multiple comparison. NS = not significant. $^{*}P < 0.05$, $^{**}P < 0.01$, $^{***}P < 0.001$. NTC = negative control; Cont Ab = isotype control monoclonal antibody; α-CXCL10 Ab = anti-CXCL10 monoclonal antibody; α-CXCR3 Ab = anti-CXCR3 monoclonal antibody.

however, the precise mechanisms by which these inflammatory lesions are formed and maintained remain unclear. We hypothesized that a positive feedback loop driven by chemokines may be responsible for the chronic inflammation associated with HAM/TSP. We identified CXCL10 as the principal chemokine responsible for inducing this chronic inflammation. We found for the first time astrocytes to be the main producers of CXCL10. Our data suggest that these astrocytes are stimulated to produce CXCL10 initially by IFN-γ released by infected T cells, where the infection appears to have produced changes in the cells that promote spontaneous IFN-γ production. In short, we inferred that spinal cord lesions found in patients with HAM/TSP arise when IFN-γ produced by HTLV-1-infected T cells induces astrocytes to secrete CXCL10, which attracts $CXCR3^{+}$ T cells, including more T cells infected with HTLV-1, thereby continuing the cycle. Furthermore, we demonstrated that an interruption of this pathway represents a promising strategy for treating HAM/TSP.

First, we identified the key chemokine involved in inducing the migration of cells to sites of inflammation. We compared the CSF and serum levels of several chemokines and demonstrated for the first time that CXCL10 is the only chemokine of those studied that is present at a significantly higher concentration in the CSF than in the sera of patients with HAM/TSP. Although previous reports indicate that CCL5 and CXCL9 levels are also elevated in the CSF of patients with HAM/TSP (Teixeira *et al.*, 2004; Tanaka *et al.*, 2008), we showed that these two chemokines exhibit a concentration gradient in the opposite direction (Fig. 1B). We previously measured the levels of other chemokines such as CCL3, CCL4, CXCL11, CCL17, CCL20 and CCL22 in the CSF and found that the levels of these chemokines are negligible in patients with HAM/TSP (Sato, in press). Importantly, we also previously demonstrated that CSF CXCL10 levels are correlated with the rate of disease progression (Sato, in press). These findings suggest that CXCL10 is crucial for the development of chronic inflammation in patients with HAM/TSP.

In the present study, we found a positive correlation between CSF CXCL10 levels and CSF cell counts (Fig. 1A), a high percentage of CXCR3-positive cells in the CSF (Fig. 2A and B; 92.4 ± 7.0%), and perivascular accumulation of $CXCR3^+$ cells in spinal cord lesions of patients with HAM/TSP (Fig. 2C). These results strongly indicate that a high concentration of CXCL10 in the spinal cord attracts $CXCR3^+$ cells that include proinflammatory cells (Qin *et al.*, 1998; Sallusto *et al.*, 1998; Thomas *et al.*, 2003). Intriguingly, the percentage of $CXCR3^+$ cells among peripheral blood mononuclear cells from patients with HAM/TSP was significantly lower than that observed in asymptomatic carriers and healthy donors, but not patients with adult T cell leukaemia (Supplementary Fig. 3). $CXCR3^+$ peripheral blood mononuclear cells are relatively few in patients with adult T cell leukaemia, perhaps because of an increase in $CCR4^+CXCR3^-$ tumour cells in the peripheral blood (Ishida *et al.*, 2003). Although the precise mechanism by which peripheral $CXCR3^+$ cells in patients with HAM/TSP become diminished remains unclear, we believe that many of these cells migrate into the CNS and contribute to the formation of spinal cord lesions. Other possible mechanisms include migration to lymphoid organs such as lymph nodes or the spleen. Because lymph nodes are important organs for CXCL10–CXCR3 interactions in patients suffering from various diseases (Groom *et al.*, 2012; Sung *et al.*, 2012), future studies analysing the lymph nodes of patients with HAM/TSP may provide a more complete understanding of HAM/TSP pathogenesis.

The discovery that CXCL10–CXCR3 interactions represent an important pathway for recruiting cells to the CNS in patients with HAM/TSP prompted us to search the spinal cord lesions of patients with HAM/TSP and identify the CXCL10-producing cells. Firstly, we confirmed that CXCL10-producing cells are more numerous in the spinal cords of patients with HAM/TSP than control individuals (Fig. 3A). We also compared high and low inflammatory regions within a single patient with HAM/TSP and found more CXCL10-producing cells in the more inflamed region (Supplementary Fig. 4), although the limitation of sampling from only a single individual prevents us from extrapolating too freely on the significance of this result. Although CXCL10 is secreted by several cell types such as monocytes, endothelial cells, fibroblasts and astrocytes in response to IFN-γ (Luster and Ravetch, 1987; Lee *et al.*, 2009), our study demonstrated that astrocytes are the major CXCL10-producing cells in thoracic spinal cord lesions in patients with HAM/TSP (Fig. 3). Notably, the astrocytes examined in this study were star-shaped with radiating cytoplasmic processes, indicating high cytological activity (Fig. 3B and C). In the CNS, CXCL10 is mainly produced by astrocytes; however, CXCL9 is primarily a product of microglial cells (Muller *et al.*, 2010). Therefore, the finding that CXCL10 production is substantially higher than CXCL9 production in the CSF (Fig. 1) suggests that astrocytes are very active in HAM/TSP. This finding supports a previous finding that gliosis is one of the main pathological features of HAM/TSP (Iwasaki, 1990; Izumo *et al.*, 1992).

Next, we investigated the mechanism by which astrocytes produce CXCL10 in patients with HAM/TSP. CXCL10 is generally not detectable in most non-lymphoid tissues under physiological conditions; however, its synthesis is easily induced by cytokines, particularly IFN-γ. Therefore, it was important to determine the source of IFN-γ that stimulates astrocytes to produce CXCL10 in patients with HAM/TSP. Interestingly, we have shown that $CD4^+$ T cells from patients with HAM/TSP spontaneously produce IFN-γ and induce CXCL10 production by U251 human astrocytoma cells via IFN-γ (Fig. 4), whereas $CD4^+$ T cells from healthy donors do not induce CXCL10 production (data not shown). These results support the hypothesis that there are interactions between HTLV-1-infected $CD4^+$ T cells and astrocytes in patients with HAM/TSP *in vivo* that may possibly initiate the first wave of CXCL10 production. Moreover, this CXCL10 production may further induce the trafficking of peripheral $CXCR3^+$ T cells. Importantly, we demonstrated that a number of peripheral $CXCR3^+$ T cells are infected with HTLV-1 (Fig. 2E), indicating that migration of peripheral $CXCR3^+$ T cells into the CNS can induce further secretion of IFN-γ that continues the vicious cycle. In fact, HTLV-1-infected $CD4^+$ T cells and IFN-γ-producing T cells have been detected in HAM/TSP spinal cord lesions (Umehara *et al.*, 1994; Moritoyo *et al.*, 1996; Matsuoka *et al.*, 1998). Notably, more than half of the $CXCR3^+$ T cells in the CSF of patients with HAM/TSP are $CD8^+$ T cells (Fig. 2D). It has been shown that $CD8^+$ cytotoxic T lymphocytes (CTLs), particularly HTLV-1-specific CTLs, have a high potential for secreting IFN-γ (Kubota *et al.*, 2000; Hanon *et al.*, 2001) and are abnormally elevated in the CSF and spinal cord lesions (Nagai *et al.*, 2001*a*, *b*; Matsuura *et al.*, 2010). Therefore, CXCL10 production by astrocytes may further boost the trafficking of $CXCR3^+$-infected $CD4^+$ T cells as well as $CXCR3^+CD8^+$ CTLs that secrete IFN-γ, leading to a positive feedback-driven chronic inflammatory loop.

The results of the present study and other studies show that the pathology of HAM/TSP is unique among immune disorders. Unlike other inflammatory disorders such as multiple sclerosis or rheumatoid arthritis that exhibit Th17 as well as Th1 involvement (Matusevicius *et al.*, 1999; Kirkham *et al.*, 2006), HAM/TSP pathogenesis appears to be dominated by the Th1 axis, particularly CXCL10–CXCR3 interactions. Our research indicates that the characteristics of HTLV-1-infected T cells may be responsible for the emphasis on the Th1 axis in HAM/TSP pathogenesis. We have reported that cultured $CD4^+$ T cells from patients with HAM/TSP clearly exhibit detectable production of IFN-γ (a Th1 cytokine) but not IL-17 (a Th17 cytokine) (Fig. 4B), and we previously demonstrated that HTLV-1-infected T cells in patients with HAM/TSP exhibit elevated IFN-γ and reduced IL-17 production (Yamano *et al.*, 2009). Furthermore, HAM/TSP peripheral blood contained more CXCL10 (Supplementary Fig. 1B) and fewer $CXCR3^+$ cells (Supplementary Fig. 3B) than asymptomatic carrier blood, suggesting that a greater number of $CXCR3^+$ cells had migrated out of the periphery due at least in part to chemotaxis induced by elevated CXCL10 production in the CNS. As the proviral loads of all the samples used in the above experiment were roughly identically high, it can be assumed that these characteristics are indeed features of HAM/TSP pathogenesis as opposed to simple consequences of having a high proviral load.

We suspect that a genetic predisposition for higher IFN-γ or CXCL10 production in response to HTLV-1 may exist. Recently, systems biology approaches were used to show that a subset of IFN-stimulated genes, including the gene encoding CXCL10, is overexpressed in peripheral blood mononuclear cells of patients with HAM/TSP compared with asymptomatic carriers

(Tattermusch *et al.*, 2012). It will be important to test for an association between genetic polymorphisms in interferon-associated genes and the presence of HAM/TSP in future studies. The existence of this genetic predisposition would strengthen the argument for Th1-dominance and explain why some infected individuals develop HAM/TSP, whereas others remain life-long asymptomatic carriers. Because it is well-known that interferons and products of interferon-stimulated genes mediate antiviral responses (Randall and Goodbourn, 2008), IFN-γ and CXCL10 production in HTLV-1-infected patients (Supplementary Fig. 1) may be considered a normal immune response. However, once the production levels surpass threshold and a CXCL10–CXCR3 amplification loop develops, it may begin to cause tissue damage. Possible reasons for CXCL10 overproduction in HAM/TSP include the presence of a high number of HTLV-1-infected T cells (Nagai *et al.*, 1998; Yamano *et al.*, 2002) and a genetic predisposition for higher IFN-γ and/or CXCL10 production in response to HTLV-1.

The ideal therapeutic strategy for treating HAM/TSP would be eradication of HTLV-1-infected cells, but this has yet to be proven possible. Another promising approach would be a receptor blockade using anti-CXCR3 neutralizing antibody, which has been reported to be effective at blocking CXCR3 activity (Van den Steen *et al.*, 2008). Although we were unable to validate this effect using our commercially available antibody, this certainly does not rule out a receptor blockade as a therapeutic candidate. Our relative success at disrupting inflammatory cell migration using anti-CXCL10 neutralizing antibodies (Fig. 5) suggests that targeting CXCL10 to interrupt the positive feedback loop may be the more promising new strategy for effectively treating HAM/TSP. A noteworthy potential advantage of anti-CXCL10 over anti-CXCR3 is that it may yield less severe side effects as only interactions with CXCL10 rather than all CXCR3 agonists would be blocked.

In conclusion, our data revealed novel insights into the pathogenic processes of HAM/TSP. Our results suggest that CXCL10 plays a pivotal role in the development of chronic inflammatory lesions where HTLV-1-infected T cells produce IFN-γ, which induces astrocytes to secrete CXCL10. This further boosts the trafficking of $CXCR3^+$-infected T cells that secrete IFN-γ, leading to a virus-induced CXCL10–CXCR3 inflammatory loop. Thus, HAM/TSP represents a pathological consequence of interactions that occur between the immune system and CNS. Understanding these complex interactions should provide new insights into the functional regulation of both systems and help uncover new therapeutic targets.

Acknowledgements

The authors thank K. Takahashi, Y. Kunitomo, Y. Sato, Y. Suzuki, M. Koike, and Y. Hasegawa for technical assistance.

Funding

This work was partly supported by project "Research on Measures for Intractable Disease," a matching fund subsidy from the Ministry of Health Labour and Welfare, a Grant-in-Aid for Scientific Research from the Ministry of Education, Culture, Sports, Science and Technology, and the MEXT-Supported Program for the Strategic Research Foundation at Private Universities, 2008–2012.

Supplementary material

Supplementary material is available at *Brain* online.

References

Furuya T, Nakamura T, Shirabe S, Nishiura Y, Tsujino A, Goto H, et al. Heightened transmigrating activity of CD4-positive T cells through reconstituted basement membrane in patients with human T-lymphotropic virus type I-associated myelopathy. Proc Assoc Am Physicians 1997; 109: 228–36.

Gessain A, Barin F, Vernant JC, Gout O, Maurs L, Calender A, et al. Antibodies to human T-lymphotropic virus type-I in patients with tropical spastic paraparesis. Lancet 1985; 2: 407–10.

Goon PK, Hanon E, Igakura T, Tanaka Y, Weber JN, Taylor GP, et al. High frequencies of Th1-type CD4(+) T cells specific to HTLV-1 env and tax proteins in patients with HTLV-1-associated myelopathy/tropical spastic paraparesis. Blood 2002; 99: 3335–41.

Groom JR, Richmond J, Murooka TT, Sorensen EW, Sung JH, Bankert K, et al. CXCR3 chemokine receptor-ligand interactions in the lymph node optimize CD4(+) T helper 1 cell differentiation. Immunity 2012; 37: 1091–103.

Hanon E, Goon P, Taylor GP, Hasegawa H, Tanaka Y, Weber JN, et al. High production of interferon gamma but not interleukin-2 by human T-lymphotropic virus type I-infected peripheral blood mononuclear cells. Blood 2001; 98: 721–6.

Hinuma Y, Nagata K, Hanaoka M, Nakai M, Matsumoto T, Kinoshita KI, et al. Adult T-cell leukemia: antigen in an ATL cell line and detection of antibodies to the antigen in human sera. Proc Natl Acad Sci USA 1981; 78: 6476–80.

Ijichi S, Eiraku N, Osame M, Izumo S, Kubota R, Maruyama I, et al. In vitro modulation of lymphocyte proliferation by prednisolone and interferon-alpha in patients with HTLV-I-associated myelopathy (HAM). J Neuroimmunol 1989; 23: 175–8.

Ishida T, Utsunomiya A, Iida S, Inagaki H, Takatsuka Y, Kusumoto S, et al. Clinical significance of CCR4 expression in adult T-cell leukemia/lymphoma: its close association with skin involvement and unfavorable outcome. Clin Cancer Res 2003; 9: 3625–34.

Itoyama Y, Minato S, Kira J, Goto I, Sato H, Okochi K, et al. Spontaneous proliferation of peripheral blood lymphocytes increased in patients with HTLV-I-associated myelopathy. Neurology 1988; 38: 1302–7.

Iwasaki Y. Pathology of chronic myelopathy associated with HTLV-I infection (HAM/TSP). J Neurol Sci 1990; 96: 103–23.

Izumo S, Ijichi T, Higuchi I, Tashiro A, Takahashi K, Osame M. Neuropathology of HTLV-I-associated myelopathy—a report of two autopsy cases. Acta Paediatr Jpn 1992; 34: 358–64.

Jacobson S, Shida H, McFarlin DE, Fauci AS, Koenig S. Circulating CD8(plus) cytotoxic T lymphocytes specific for HTLV-I pX in patients with HTLV-I associated neurological disease. Nature 1990; 348: 245–8.

Jeffery KJ, Usuku K, Hall SE, Matsumoto W, Taylor GP, Procter J, et al. HLA alleles determine human T-lymphotropic virus-I (HTLV-I) proviral load and the risk of HTLV-I-associated myelopathy. Proc Natl Acad Sci USA 1999; 96: 3848–53.

Kirkham BW, Lassere MN, Edmonds JP, Juhasz KM, Bird PA, Lee CS, et al. Synovial membrane cytokine expression is predictive of joint damage progression in rheumatoid arthritis: a two-year prospective study (the DAMAGE study cohort). Arthritis Rheum 2006; 54: 1122–31.

Kubota R, Kawanishi T, Matsubara H, Manns A, Jacobson S. HTLV-I specific IFN-gamma+ CD8+ lymphocytes correlate with the proviral load in peripheral blood of infected individuals. J Neuroimmunol 2000; 102: 208–15.

Lee EY, Lee ZH, Song YW. CXCL10 and autoimmune diseases. Autoimmun Rev 2009; 8: 379–83.
Libby P. Inflammation in atherosclerosis. Nature 2002; 420: 868–74.
Luster AD. Chemokines—chemotactic cytokines that mediate inflammation. N Engl J Med 1998; 338: 436–45.
Luster AD, Ravetch JV. Biochemical characterization of a gamma interferon-inducible cytokine (IP-10). J Exp Med 1987; 166: 1084–97.
Mantovani A, Allavena P, Sica A, Balkwill F. Cancer-related inflammation. Nature 2008; 454: 436–44.
Matsuoka E, Takenouchi N, Hashimoto K, Kashio N, Moritoyo T, Higuchi I, et al. Perivascular T cells are infected with HTLV-I in the spinal cord lesions with HTLV-I-associated myelopathy/tropical spastic paraparesis: double staining of immunohistochemistry and polymerase chain reaction in situ hybridization. Acta Neuropathol 1998; 96: 340–6.
Matsuura E, Yamano Y, Jacobson S. Neuroimmunity of HTLV-I infection. J Neuroimmune Pharmacol 2010; 5: 310–25.
Matusevicius D, Kivisakk P, He B, Kostulas N, Ozenci V, Fredrikson S, et al. Interleukin-17 mRNA expression in blood and CSF mononuclear cells is augmented in multiple sclerosis. Mult Scler 1999; 5: 101–4.
Medzhitov R. Inflammation 2010: new adventures of an old flame. Cell 2010; 140: 771–6.
Medzhitov R. Origin and physiological roles of inflammation. Nature 2008; 454: 428–35.
Moritoyo H, Arimura K, Arimura Y, Tokimura Y, Rosales R, Osame M. Study of lower limb somatosensory evoked potentials in 96 cases of HTLV-I-associated myelopathy/tropical spastic paraparesis. J Neurol Sci 1996; 138: 78–81.
Muller M, Carter S, Hofer MJ, Campbell IL. Review: the chemokine receptor CXCR3 and its ligands CXCL9, CXCL10 and CXCL11 in neuroimmunity—a tale of conflict and conundrum. Neuropathol Appl Neurobiol 2010; 36: 368–87.
Nagai M, Yamano Y, Brennan MB, Mora CA, Jacobson S. Increased HTLV-I proviral load and preferential expansion of HTLV-I tax-specific CD8+ T cells in cerebrospinal fluid from patients with HAM/TSP. Ann Neurol 2001a; 50: 807–12.
Nagai M, Brennan MB, Sakai JA, Mora CA, Jacobson S. CD8(+) T cells are an *in vivo* reservoir for human T-cell lymphotropic virus type I. Blood 2001b; 98: 1858–61.
Nagai M, Usuku K, Matsumoto W, Kodama D, Takenouchi N, Moritoyo T, et al. Analysis of HTLV-I proviral load in 202 HAM/TSP patients and 243 asymptomatic HTLV-I carriers: high proviral load strongly predisposes to HAM/TSP. J Neurovirol 1998; 4: 586–93.
Narikawa K, Fujihara K, Misu T, Feng J, Fujimori J, Nakashima I, et al. CSF-chemokines in HTLV-I-associated myelopathy: CXCL10 up-regulation and therapeutic effect of interferon-alpha. J Neuroimmunol 2005; 159: 177–82.
Nie CQ, Bernard NJ, Norman MU, Amante FH, Lundie RJ, Crabb BS, et al. IP-10-mediated T cell homing promotes cerebral inflammation over splenic immunity to malaria infection. PLoS Pathog 2009; 5: e1000369.
Osame M. Review of WHO kagoshima meeting and diagnostic guidelines for HAM/TSP. In: Blattner WA, editor. Human retrovirology: HTLV. New York: Raven Press, 1990. p. 191–7.
Osame M, Usuku K, Izumo S, Ijichi N, Amitani H, Igata A, et al. HTLV-I associated myelopathy, a new clinical entity. Lancet 1986; 1: 1031–2.
Proost P, Vynckier AK, Mahieu F, Put W, Grillet B, Struyf S, et al. Microbial toll-like receptor ligands differentially regulate CXCL10/IP-10 expression in fibroblasts and mononuclear leukocytes in synergy with IFN-gamma and provide a mechanism for enhanced synovial chemokine levels in septic arthritis. Eur J Immunol 2003; 33: 3146–53.
Proost P, Schutyser E, Menten P, Struyf S, Wuyts A, Opdenakker G, et al. Amino-terminal truncation of CXCR3 agonists impairs receptor signaling and lymphocyte chemotaxis, while preserving antiangiogenic properties. Blood 2001; 98: 3554–61.
Qin S, Rottman JB, Myers P, Kassam N, Weinblatt M, Loetscher M, et al. The chemokine receptors CXCR3 and CCR5 mark subsets of T cells associated with certain inflammatory reactions. J Clin Invest 1998; 101: 746–54.
Randall RE, Goodbourn S. Interferons and viruses: an interplay between induction, signalling, antiviral responses and virus countermeasures. J Gen Virol 2008; 89: 1–47.
Richardson JH, Edwards AJ, Cruickshank JK, Rudge P, Dalgleish AG. *In vivo* cellular tropism of human T-cell leukemia virus type 1. J Virol 1990; 64: 5682–7.
Saito M, Bangham CR. Immunopathogenesis of human T-cell leukemia virus type-1-associated myelopathy/tropical spastic paraparesis: recent perspectives. Leuk Res Treatment 2012; 2012: 259045.
Sallusto F, Lenig D, Mackay CR, Lanzavecchia A. Flexible programs of chemokine receptor expression on human polarized T helper 1 and 2 lymphocytes. J Exp Med 1998; 187: 875–83.
Shimoyama M. Diagnostic criteria and classification of clinical subtypes of adult T-cell leukaemia-lymphoma. A report from the lymphoma study group (1984–87). Br J Haematol 1991; 79: 428–37.
Sung JH, Zhang H, Moseman EA, Alvarez D, Iannacone M, Henrickson SE, et al. Chemokine guidance of central memory T cells is critical for antiviral recall responses in lymph nodes. Cell 2012; 150: 1249–63.
Tanaka M, Matsushita T, Tateishi T, Ochi H, Kawano Y, Mei FJ, et al. Distinct CSF cytokine/chemokine profiles in atopic myelitis and other causes of myelitis. Neurology 2008; 71: 974–81.
Tattermusch S, Skinner JA, Chaussabel D, Banchereau J, Berry MP, McNab FW, et al. Systems biology approaches reveal a specific interferon-inducible signature in HTLV-1 associated myelopathy. PLoS Pathog 2012; 8: e1002480.
Teixeira AL Jr, Cardoso F, Souza AL, Teixeira MM. Increased serum concentrations of monokine induced by interferon-gamma/CXCL9 and interferon-gamma-inducible protein 10/CXCL-10 in sydenham's chorea patients. J Neuroimmunol 2004; 150: 157–62.
Thomas SY, Hou R, Boyson JE, Means TK, Hess C, Olson DP, et al. CD1d-restricted NKT cells express a chemokine receptor profile indicative of Th1-type inflammatory homing cells. J Immunol 2003; 171: 2571–80.
Umehara F, Izumo S, Ronquillo AT, Matsumuro K, Sato E, Osame M. Cytokine expression in the spinal cord lesions in HTLV-I-associated myelopathy. J Neuropathol Exp Neurol 1994; 53: 72–7.
Van den Steen PE, Deroost K, Van Aelst I, Geurts N, Martens E, Struyf S, et al. CXCR3 determines strain susceptibility to murine cerebral malaria by mediating T lymphocyte migration toward IFN-gamma-induced chemokines. Eur J Immunol 2008; 38: 1082–95.
Waldmann TA. The biology of interleukin-2 and interleukin-15: implications for cancer therapy and vaccine design. Nat Rev Immunol 2006; 6: 595–601.
Yamano Y, Sato T. Clinical pathophysiology of human T-lymphotropic virus-type 1-associated myelopathy/tropical spastic paraparesis. Front Microbiol 2012; 3: 389.
Yamano Y, Takenouchi N, Li HC, Tomaru U, Yao K, Grant CW, et al. Virus-induced dysfunction of CD4+CD25+ T cells in patients with HTLV-I-associated neuroimmunological disease. J Clin Invest 2005; 115: 1361–8.
Yamano Y, Nagai M, Brennan M, Mora CA, Soldan SS, Tomaru U, et al. Correlation of human T-cell lymphotropic virus type 1 (HTLV-1) mRNA with proviral DNA load, virus-specific CD8(+) T cells, and disease severity in HTLV-1-associated myelopathy (HAM/TSP). Blood 2002; 99: 88–94.
Yamano Y, Araya N, Sato T, Utsunomiya A, Azakami K, Hasegawa D, et al. Abnormally high levels of virus-infected IFN-gamma+ CCR4+ CD4+ CD25+ T cells in a retrovirus-associated neuroinflammatory disorder. PLoS One 2009; 4: e6517.
Yasuda N, Lai PK, Ip SH, Kung PC, Hinuma Y, Matsuoka M, et al. Soluble interleukin 2 receptors in sera of japanese patients with adult T cell leukemia mark activity of disease. Blood 1988; 71: 1021–6.

The American Journal of Pathology, Vol. 182, No. 5, May 2013

ELSEVIER

The American Journal of
PATHOLOGY

ajp.amjpathol.org

TUMORIGENESIS AND NEOPLASTIC PROGRESSION

Protective Roles of Epithelial Cells in the Survival of Adult T-Cell Leukemia/Lymphoma Cells

Yukiko Miyatake,*† André L.A. Oliveira,†‡ Mohamed Ali Jarboui,† Shuichi Ota,§ Utano Tomaru,* Takanori Teshima,¶ William W. Hall,† and Masanori Kasahara*

From the Departments of Pathology and Hematology,¶ Hokkaido University Graduate School of Medicine, Sapporo, Japan; the Centre for Research in Infectious Diseases,† School of Medicine and Medical Science, University College Dublin, Dublin, Ireland; ICON Central Laboratories,‡ Dublin, Ireland; and the Department of Hematology,§ Sapporo Hokuyu Hospital, Sapporo, Japan*

Accepted for publication January 10, 2013.

Address correspondence to Yukiko Miyatake, Ph.D., Department of Pathology, Hokkaido University Graduate School of Medicine, Kita-15, Nishi-7, Kita-ku, Sapporo 060-8638, Japan. E-mail: yukimiya@med.hokudai.ac.jp.

Adult T-cell leukemia/lymphoma (ATL) is a highly invasive and intractable T-cell malignancy caused by human T-cell leukemia virus-1 infection. We demonstrate herein that normal tissue–derived epithelial cells (NECs) exert protective effects on the survival of leukemic cells, which may partially account for high resistance to antileukemic therapies in patients with ATL. Viral gene–silenced, ATL-derived cell lines (ATL cells) dramatically escaped from histone deacetylase inhibitor–induced apoptosis by direct co-culture with NECs. Adhesions to NECs suppressed $p21^{Cip1}$ expression and increased a proportion of resting G0/G1 phase cells in trichostatin A (TSA)–treated ATL cells. ATL cells adhering to NECs down-regulated CD25 expression and enhanced vimentin expression, suggesting that most ATL cells acquired a quiescent state by cell-cell interactions with NECs. ATL cells adhering to NECs displayed highly elevated expression of the cancer stem cell marker CD44. Blockade of CD44 signaling diminished the NEC-conferred resistance of ATL cells to TSA-induced apoptosis. Co-culture with NECs also suppressed the expression of NKG2D ligands on TSA-treated ATL cells, resulting in decreased natural killer cell–mediated cytotoxicity. Combined evidence suggests that interactions with normal epithelial cells augment the resistance of ATL cells to TSA-induced apoptosis and facilitate immune evasion by ATL cells. *(Am J Pathol 2013, 182: 1832–1842; http://dx.doi.org/10.1016/j.ajpath.2013.01.015)*

Adult T-cell leukemia/lymphoma (ATL) is an intractable and fatal T-cell malignancy caused by human T-cell leukemia virus type 1 (HTLV-1).[1] After more than two decades of long-term latency, approximately 4% of HTLV-1 carriers develop ATL.[2,3] A striking feature of ATL is aggressive invasion of leukemia cells into the skin and epithelial linings of the gastrointestinal tract and lung.[4,5] Leukemia cells that have invaded the tissues are resistant to chemotherapy, presenting a major obstacle to the effective treatment of ATL.[6] Therefore, understanding the mechanisms by which tissue-infiltrating leukemia cells acquire resistance to chemotherapy is key to developing new promising treatments for patients with ATL.

HTLV-1 proteins are generally undetectable in HTLV-1–infected cells isolated from HTLV-1 carriers because of viral gene silencing. Such silencing is observed not only in asymptomatic carriers but also in patients with ATL, indicating that it allows ATL cells to evade the host immune response *in vivo*.[7,8] However, the mechanisms leading to viral gene silencing are poorly understood. Freshly isolated HTLV-1–infected cells begin to express viral genes after overnight culture *in vitro*, implying that an unknown mechanism exists to suppress viral genes *in vivo*.[9] Recently, primary ATL cells were shown to be well maintained *in vitro* by co-culture in direct contact with stromal cells.[10] Furthermore, type I interferon–induced HTLV-1 *gag* expression was suppressed in an ATL cell line when it was co-cultured with stromal cells.[11] These observations suggest that viral gene silencing occurs in ATL cells by interactions with the host microenvironment.

Epigenetic regulations, such as histone acetylation, are also assumed to be involved in viral gene silencing in ATL

Supported by Grants-in-Aid for Young Scientists from the Ministry of Education, Culture, Sports, Science and Technology of Japan and the Centre for Research in Infectious Diseases, School of Medicine and Medical Science, University College Dublin.

http://dx.doi.org/10.1016/j.ajpath.2013.01.015

cells.[12] Thus, the *trans*-activity of the HTLV-1 long terminal repeats (LTRs) is induced by histone deacetylase (HDAC) inhibitors in HTLV-1–infected MT4 cells.[13] Also, HTLV-1 Tax expression was doubled when primary ATL cells were treated with HDAC inhibitors.[14] These observations indicate that in ATL cells cultured *in vitro*, viral gene expression is suppressed by epigenetic regulation and that HDAC inhibitors can reactivate silenced viral genes. Taken together, available evidence indicates that viral gene expression is suppressed in ATL cells by the dual action of the microenvironment of the host-tumor interface and epigenetic regulation in host cells.

Stromal fibroblasts constituting the bone marrow microenvironment prevent chemotherapy-induced apoptosis in acute myeloid leukemia and chronic lymphocytic leukemia cells.[15,16] Recently, stromal cell–derived factor-1α and its cognate receptor CXCR4 have emerged as critical mediators of leukemic/stromal cell interactions.[17] Blockade of the stromal cell–derived factor-1α–CXCR4 axis by the CXCR4 antagonist AMD3100 suppresses the migration of cultured ATL cells,[18] suggesting that this axis may also be involved in formation of the stromal niche environment in ATL.

The present study was undertaken to determine whether epithelial cells, another major component constituting the microenvironment of the host-tumor interface, affect the survival and phenotype of ATL cells. We show that co-culture with normal tissue–derived epithelial cells (NECs) increases a proportion of ATL cells in G0/G1 phase and rescues ATL cells from HDAC inhibitor–induced apoptosis. Adhesions to NECs induced prominent surface expression of CD44 on ATL cells; they also induced internalization of CD44 and nuclear translocation of cyclin D1 in a fraction of HDAC inhibitor–treated ATL cells, thus enabling such ATL cells to resume cell-cycle progression and leading to the ultimate survival of ATL cells. ATL cells co-cultured with NECs down-regulated the expression of NKG2D ligands, suggesting that this interaction also facilitates immune evasion by tumor cells.

Materials and Methods

Cells

The HTLV-1–positive ATL cell lines ATL-CR and ATL-TH were obtained from the Reference Center for HTLV Infection (Rio de Janeiro, Brazil). These cell lines were established from Brazilian patients with ATL after they provided informed consent. Briefly, peripheral blood mononuclear cells (PBMCs) isolated from patients with ATL were cultured in the presence of recombinant IL-2. After long-term culture, they acquired IL-2 independence, resulting in establishment of the ATL-CR and ATL-TH cell lines. Jurkat and HUT78, a T-cell lymphoma line derived from a patient with Sezary syndrome,[19] were used as HTLV-1–negative T-cell lymphoma cells. ATL-CR, ATL-TH, Jurkat, and HUT78 were maintained in RPMI 1640 medium supplemented with 10% fetal bovine serum (FBS) and penicillin/streptomycin. HEK293 and HEK293T, human embryo kidney epithelial-like cell lines, and primary normal human dermal fibroblasts were maintained in Dulbecco's minimal essential medium supplemented with 10% FBS and penicillin/streptomycin. 1C3IKEI, a primary normal human embryonic pancreas–derived epithelial-like cell line, was purchased from the RIKEN BioResource Center (Tsukuba, Japan) and maintained in Dulbecco's minimal essential medium supplemented with 15% FBS. KHYG-1, an NKG2D$^+$ natural killer (NK) cell line,[20] was purchased from the Health Science Research Resources Bank (Osaka, Japan) and was maintained in Dulbecco's minimal essential medium supplemented with 100 U of recombinant human IL-2 (Shionogi, Osaka, Japan), 10% FBS, and penicillin/streptomycin. Fresh ATL cells were obtained from patients with chronic or acute ATL after informed consent was provided. Briefly, PBMCs isolated from heparinized peripheral blood by Ficoll-Paque PLUS (GE Healthcare Life Sciences, Little Chalfont, UK) were resuspended in RPMI 1640 medium supplemented with 10% FBS and penicillin/streptomycin and were subjected to experiments immediately.

Antibodies, Plasmids, and Reagents

Rat anti-human/mouse CD44 antibody (clone IM7; eBioscience Inc., San Diego, CA) was used for flow cytometry (FCM) and immunofluorescence staining. Mouse anti-human MICA/B antibody (clone 6D4; eBioscience) was used for FCM. Mouse anti-human CD25 (clone BC96; eBioscience), polyclonal rabbit anti-human fibronectin (Dako, Glostrup, Denmark), mouse anti-human vimentin (clone V9; Dako), polyclonal rabbit anti-human $p21^{Cip1}$ (eBioscience), and mouse anti-human Ki-67 (clone MIB-1; Dako) antibodies were used for immunofluorescence staining. HTLV-1 LTR luciferase plasmids have been described previously.[21] HDAC inhibitors, such as trichostatin A (TSA), valproic acid sodium salt (VPA), and sodium butyrate (NaB), were purchased from Sigma-Aldrich (St. Louis, MO).

Co-Culture

ATL cells were co-cultured with NECs using a direct co-culture system that allowed for cell-cell contact. NECs were labeled with 1 μmol/L of 5- (and 6-) carboxyfluorescein diacetate succinimidyl ester (CFSE) at a concentration of 1×10^6 cells/mL in PBS for 20 minutes at 37°C and then washed three times in PBS. CFSE-labeled NECs were used immediately for each experiment. ATL cells, 5×10^5, were directly co-cultured with CFSE-labeled NECs growing as monolayers in 24-well plates. Cell culture inserts (pore size, 0.4 μm; Invitrogen, Camarillo, CA) were used for an indirect co-culture system. ATL cells were co-cultured with CFSE-labeled NECs using the indicated concentrations of TSA. After the indicated co-culture time, whole cells in co-culture were harvested for subsequent experiments. In some experiments, nonadhering ATL cells in the supernatant were collected separately from the ATL cells adhering to the